Arabidopsis ABA-activated kinase MAPKKK18 is regulated by protein phosphatase 2C ABI1 and the ubiquitin proteasome pathway

Running title: MKKK18 is regulated by ABI1 and proteasome

Corresponding author: Agnieszka Ludwików

Department of Biotechnology, Institute of Molecular Biology and Biotechnology

Faculty of Biology, Adam Mickiewicz University in Poznań, ul. Umultowska 89, Collegium Biologicum, 61-614 Poznań, Poland

tel. (48) 61 8295964; fax. (48) 61 8295949; ludwika@amu.edu.pl

Subject areas:

1. proteins, enzymes and metabolism

Arabidopsis ABA-activated kinase MAPKKK18 is regulated by protein phosphatase 2C ABI1 and the ubiquitin proteasome pathway

Running title: MKKK18 is regulated by ABI1 and proteasome

Filip Mituła[1], Małgorzata Tajdel[1], Agata Cieśla[1], Anna Kasprowicz-Maluśki[2], Anna Kulik[4], Danuta Babula-Skowrońska[3], Michał Michalak[2], Grażyna Dobrowolska[4], Jan Sadowski[1] and Agnieszka Ludwików[1],

[1]Department of Biotechnology, Institute of Molecular Biology and Biotechnology, Faculty of Biology, Adam Mickiewicz University in Poznań, Umultowska 89, 61-614 Poznań, Poland

[2]Department of Molecular and Cellular Biology, Institute of Molecular Biology and Biotechnology, Faculty of Biology, Adam Mickiewicz University in Poznań, Umultowska 89, 61-614 Poznań, Poland

[3]Institute of Plant Genetics Polish Academy of Science, Strzeszyńska 34, 60-479 Poznań, Poland

[4]Institute of Biochemistry and Biophysics, Polish Academy of Sciences, Pawińskiego 5a, 02-106 Warsaw, Poland

Abreviations

ABA- abscisic acid

ABI1 – Abscisic acid insensitive 1

ABI2 – Abscisic acid insensitive 2

ABRE - ABA-responsive element

ACS/ACC synthase - Aminocyclopropane-1-carboxylic acid synthase

AD – activation domain

ASF1 - Histone chaperone

BD – binding domain

BiFC - Bimolecular fluorescence complementation

CBP20- Cap Binding Protein 20

CIPK – Calcium-induced protein kinase

DDO - SD medium without Leucine and Tryptophan

DRE - dehydration-responsive element

GC – guard cells

GFP – green fluorescent protein

GUS - beta-glucuronidase reporter gene

HAB1 – Hypersensitive to Abscisic acid 1

His - histidine tag

JNK - c-Jun N-terminal kinase

MAPK/MPK – MAP kinase

MAPKKK18 - Map kinase kinase kinase 18

MKK – MAP kinase kinase

MKKK/MEKK – MAP kinase kinase kinase

MKKK18oe – transgenic overexpresor line

MS - Murashige_and_Skoog medium

PC –pavement cells

PCR - polymerase chain reaction

PP2C- protein phosphatase type 2C

PYR/PYL/RCAR – Pyrabactin resistance1 (PYR1)/PYR1-like (PYL)/Regulatory Components of Abscisic acid Receptors (RCAR)

QDO - SD medium without Leucine, Tryptophan, Histidine or Adenine

qPCR - quantitative real-time PCR

ROS - reactive oxygen species

SD – synthetic dropout medium

SI - stomatal index

SnRK - sucrose nonfermenting (SNF)-related kinase

W-box – WRKY binding element

WT Col-0 –wild type *Arabidopsis thaliana* Columbia (Col-0/4, alias Col-4)

X-alpha-Gal - 5-bromo-4-chloro-3-indolyl alpha-D-galactopyranoside

YDA/YODA – MAP kinase kinase kinase 4, MAPKKK4

Arabidopsis ABA-activated kinase MAPKKK18 is regulated by protein phosphatase 2C ABI1 and the ubiquitin proteasome pathway

ABSTRACT

Phosphorylation and dephosphorylation events play an important role in the transmission of the abscisic acid signal. Although SnRK2 protein kinases and group A PP2C-type phosphatases constitute a core ABA pathway, little is known about the interplay between MAP kinases and protein phosphatases 2C in the regulation of ABA pathways. In this study, an effort was made to elucidate the role of MKKK18 in relation to ABA signaling and response. The MKKK18 knockout lines showed more vigorous root growth, decreased abaxial stomatal index, and increased stomatal aperture under normal growth conditions, compared to the control WT Col-0 line. In addition to transcriptional regulation of the MKKK18 promoter by ABA, we demonstrated by using *in vitro* and *in vivo* kinase assays that the kinase activity of MKKK18 was regulated by ABA and in response to H_2O_2 treatment. Analysis of the cellular localization of MKKK18 showed that the active kinase was targeted specifically to the nucleus. Notably, we identified ABI1 PP2C as a MKKK18-interacting protein, and demonstrated that ABI1 inhibited its activity. Using a cell-free degradation assay, we also established that MKKK18 was unstable and was degraded by the proteasome pathway. The rate of MKKK18 degradation was delayed in the *ABI1* knockout line. Overall, we provide evidence that ABI1 regulates activity and promotes proteasomal degradation of MKKK18.

KEYWORDS: *Arabidopsis thaliana*, MAP kinase cascade, MKKK18, ABI1 PP2C, ABA signaling, proteasome

INTRODUCTION

The phytohormone ABA recruits many diverse elements for the generation and transmission of endogenous signals (Xiong et al., 2002; Fujita et al., 2009; Ludwików et al., 2009; Santiago et al., 2009; Geiger et al., 2009; Yoshida et al., 2010; Nishimura et al., 2009; Mane et al., 2007). Protein kinases and protein phosphatases are proteins that lead to rearrangements in the network of ABA signal transduction (Ma et al., 2009; Park et al., 2009; Umezawa et al., 2009; Santiago et al., 2009; Nishimura et al., 2010; Szostkiewicz et al., 2010; Nakashima et al., 2009; Zhu et al., 2007; Ohta et al., 2003; Dupeux et al., 2011). Both protein kinases and protein phosphatases are obligatory for ABA signal transduction. SNF1-related protein kinases 2 (SnRK2s), Ca^{2+}- dependent protein kinases (CDPKs), and CBL-binding protein kinases (CIPKs) are all known for their involvement in ABA signaling and stress tolerance, and are identified as interacting partners with particular PP2Cs (Umezawa et al., 2009; Zhu et al., 2007; Ohta et al., 2003). Key players of ABA signaling such as ABI1, ABI2, and HAB1 have been shown to interact with PYR/PYL/RCAR putative ABA receptors to regulate SnRK kinases (Umezawa et al., 2009). ABI1 and ABI2, along with CIPK20, CIPK8, CIPK14, and CIPK15, manage protein-protein interactions and regulate ABA signaling, gene expression, and stress response (Guo et al., 2002; Ohta et al., 2003; Ludwików et al., 2013). Other interacting partners with PP2Cs include transcription factors (Himmelbach et al., 2002), antioxidant enzymes (Miao et. al., 2006), constituents of chromatin remodeling complex (Saez et al., 2008), and components of the ethylene biosynthetic pathway (Ludwików et al., 2014), which have likewise been identified as important to the ABA signaling network.

Despite studies indicating that MAP kinase cascades are important for ABA signaling, little is known about the interplay between MAP kinases and protein phosphatases 2C in this pathway. A MAP kinase cascade is a conserved module comprised of at least three elements:

MKKKs, MKKs, and MAPKs. A group of MKKKKs have also been identified (Jonak et al., 2002; Yoon et al., 2010). MKKKs link upstream receptors with downstream MKKs. MKKKs phosphorylate (as dual specificity kinases) on Ser/Thr residues of MKKs in conserved S/T-X3-5-S/T motifs localized in an activation loop (T-loop). Once activated, the MKKs phosphorylate MAPKs at the TxY motif located in their T-loop. Upon activation, the MAPKs phosphorylate downstream substrates, thereby initiating various cellular responses. Among the MAPKs, MPK6 is known to interact with ABI1 PP2C. Both ABI1 and MPK6 are involved in the regulation of biotic and abiotic stress responses (Leung et al., 2006). In addition, MPK3, MPK6, MPK9 and MPK12 have been identified as regulators of ABA signaling in guard cells (Lampard et al., 2009; Brock et al., 2010; Jammes et al., 2011; Salam et al., 2013). MKK1-MPK6 were found to be transiently activated by ABA treatment, to affect downstream generation of H_2O_2, and to regulate guard-cell aperture (Xing et al., 2008). Other kinases, such as MPK9 and MPK12, act upstream of anion channels in guard-cell ABA signaling (Jammes et al., 2009). In addition, MKK7 and MKK9 are known as regulators during stomatal development (Lampard et al., 2009).

Because MKKKs constitute the largest and most complex group of MAP cascade kinases, only a few MPK modules have been recognized and documented. ROS signaling in plants involves the MEKK1-MKK2-MPK4 phosphorylation pathway (Colcombet and Hirt, 2009; Pitzschke et al., 2009). In apple, the cascade MdMKK1-MdMPK1 is activated by ABA (Wang et al., 2010). In Arabidopsis, an unknown MKKK-MKK4/5-MPK3/6 module, and MEKK1-MKK1/2-MPK4, are two MAP cascades that govern flg22-dependent gene expression (Suarez-Rodriguez et al., 2007; Nicaise et al., 2009; Qiu et al., 2008; Boudsocq et al., 2010; Kong et al., 2012). Another MAP kinase cascade consists of YDA activating MKK4/5-MKK7/MKK9 and MPK3/6: the YDA module is an important protein complex that regulates stomatal development and affects influorescence architecture by promoting cell

proliferation (Wang et al., 2007; Lampard et al., 2009; Meng et al., 2012). Very recently, a MAPK cascade MAP3K17/18-MKK3-MPK1/2/7/14 was identified to play a role in ABA stress signalling (Danquah et al., 2015) and senescence (Matsuoka et al., 2015).

In this study, we investigated the role of MKKK18 in ABA signaling and response. We find that MKKK18 is regulated both by protein phosphatase 2C ABI1 and the proteasome pathway.

RESULTS

MKKK18 expression is induced by ABA

Previous studies have identified that *MKKK18* expression is increased in response to wounding (Taki et al., 2005), pathogen attack (de Torres-Zabala et al., 2007), ozone, mannitol, NaCl and ABA treatment (Hoth et al., 2002; Leonhardt et al., 2004; Ludwików et al., 2009; Danquah et al., 2015). The responsiveness of the *MKKK18* promoter to ABA, quinabactin (a sulfonamide ABA agonist), and ASn compounds (ABA analogs) was also demonstrated (Okamoto et al., 2013; Takeuchi et al., 2014). In addition, *MKKK18* expression was found to be deregulated in *abi1-1* and *abi1td* mutants (Hoth et al., 2002; Ludwików et al., 2009). The expression of *MKKK18* was diminished in *abi1td* (Ludwików et al., 2009), abolished in ABA-insensitive *abi1-1* mutant (Hoth et al., 2002) suggesting that the proper transcription of *MKKK18* requires regular ABA signaling.

To gain a more detailed insight into the *MKKK18* gene-expression profile, we analyzed public transcriptome data compiled by Genevestigator and eFP Browser. The result indicated that *MKKK18* exhibits low-level expression in a range of plant tissues, with the exception of anthers. A relatively high-level of expression was observed in root cells, including the epidermis, endodermis, stele, cortex, and lateral root cap. A significant increase in *MKKK18*

gene expression was observed in guard cells and mesophyll cells in response to ABA treatment.

To verify the ABA responsiveness of *MKKK18*, we studied promoter activity in the 1622-bp upstream region of the *MKKK18* gene in transgenic plants carrying promoters fused with GUS reporter genes. A *de novo* search for *cis*-acting elements using the PLACE program revealed that the *MKKK18* promoter contained a number of *cis*-regulatory elements. These elements included ABRE (PyACGTGGC) and DRE elements (TACCGACAT) (Yamaguchi-Shinozaki et al., 2005), an ASF1 regulatory sequence (Krawczyk et al., 2002), POLLENLELAT52 (Bate and Twell, 1998), a W-box (Yamasaki et al., 2012), and a TAAAG element required for guard-cell specific gene expression (Plesch et al, 2001). Twenty four hours after the ABA treatment, a full-length Pro*MKKK18*:GUS construct delivered strong GUS expression in the flowers, leaves and root tissues (Fig. 1). In developing flowers, MKKK18 promoter activity was observed in sepals, anther filaments, ovaries and meristem tissues (Fig. 1C-F). GUS staining was visible in root meristem tissues and in areas of lateral root formation (Fig. 1G). Pro*MKKK18*:GUS staining was observed in guard cells and trichomes (Fig. 1H-I). Our results demonstrate that a 1.6 kb upstream sequence was sufficient for MKKK18 regulation by ABA.

Active MKKK18 is localized in the nucleus

To determine MKKK18 protein localization *in vivo,* C-terminal GFP fusions were generated and transiently expressed under the control of the *35S* promoter in *A. thaliana* protoplasts. MKKK18 was predominantly localized in the nucleus, whereas as expected empty vector did not display background fluorescence in the cytoplasm (Fig. 2A). Next, we addressed whether kinase activity affected MKKK18 localization. By multi-sequence alignment of Arabidopsis MAPKKK we identified conserved residues important for the activity of MKKK18. Based on

this analysis a kinase-inactive allele (*K32M*) and permanently active form of MKKK18 (*T161E*) were generated. A modified K32M version of the protein possessed a point mutation in its ATP-binding loop. Permanently active form of MKKK18 was obtained by substitution of conserved threonine (T) to glutamic acid (E) in positions 161 localized in the kinase domain. All versions of MKKK18 were fused to GFP and were again expressed in *Arabidopsis* protoplasts. Interestingly, the *K32M* allele showing retained barely detectable kinase activity was localized in out of the nuclei, in the cytoplasm. The fluorescent signal of the permanently active T161E version of MKKK18-GFP clearly accumulated in the nucleus of *Arabidopsis* protoplasts, suggesting a role in mediating the signaling function of MKKK18 in this compartment (Fig. 2A). Immunoblot analysis confirmed the presence of full-length fusion proteins (Fig. 2B).

MKKK18-overexpressing lines show ABA-related phenotypes at the level of germination and root growth

To investigate the functions of MKKK18, six independent *MKKK18*-overexpressor lines (Col-0*/35S:MKKK18-GFP*; *MKKK18oe1-6*) were generated and two T-DNA insertion lines of *MKKK18* in the Col background were selected from the SALK and GABI-Kat collections. These knockout lines were designated *mkkk18-1* (SALK_087047) and *mkkk18-2* (GK-244G02). Homozygous *mkkk18-1* and *mkkk18-2* plants were identified by PCR-based genotyping, and the insertion site was confirmed by PCR using T-DNA specifics and gene specific primers (Fig. 3A-B). A qPCR analysis confirmed that expression of MKKK18 was abolished in both *mkkk18-2* and *mkkk18-1* (Fig. 3C). The MKKK18 immunocomplex assay confirmed that both knockout lines were deficient in MKKK18 activity (Fig. 5).

Previous reports showed that MKKK18 is an ABA-activated kinase (Danquah et al., 2015, Matsuoka et al., 2015). To monitor the activation of ABA signaling in the leaves of the

knockouts and *MKKK18*-overexpressor lines at the molecular level, the expression of an ABA-induced genes, *RD29B* and *RAB18*, was examined by quantitative real-time PCR (Fig. 3D). In response to treatment with ABA, *RD29B* and *RAB18* expression was significantly downregulated in both *MKKK18* knockout lines than that in *MKKK18oe* and WT plants ($P < 0.001$) suggesting that the ABA-mediated induction of these genes is regulated by MKKK18. Furthermore, in the search for ABA-related phenotypes in the *MKKK18* mutants, we first analyzed whether seed germination and root growth were affected by ABA. Seeds of MKKK18*oe* lines and *mkkk18* knockouts were sown on MS medium supplemented with ABA, and the germination rate was analyzed and compared with wild-type seeds. As indicated in Figure 3E, both knockout lines showed similar growth rates to WT Col-0 in the presence of low concentrations of ABA. In contrast, Col-0*/35S:MKKK18-GFP* germinated better than the WT Col-0 control, which was supported by the *t*-test results ($P < 0.001$) between the WT and independent *MKKK18oe* lines. This observation indicated that the *35S:MKKK18-GFP*-overexpressing line displayed insensitivity towards ABA at the level of germination, suggesting that MKKK18 was required for germination. Next, in the search for ABA-related phenotypes, we analyzed ABA-mediated inhibition of root expansion. In the presence of 2 μM ABA, root elongation in seedlings expressing *35S:MKKK18-GFP* was reduced by 15% compared to the WT Col-0 control seedlings (n = 46; $P < 0.0001$). At the same ABA level, the *mkkk18-1* and *mkkk18-2* knockout lines showed improved root growth (40% and 20%, respectively) compared to the WT Col-0 line (Fig. 3F).

MKKK18 affects stomatal development and function

MAP kinases are important elements of signaling cascades that affect stomatal development (Wang et al., 2007; Lampard et al., 2009; Tanaka et al., 2013). Therefore, we compared the number and density of stomata in 6- and 10-day-old seedlings of both *MKKK18*-

overexpressing lines and *MKKK18* knockout lines (Fig. 4A). In the cotyledons, the SI was significantly reduced by 19% and 26%, for *mkkk18-1* ($P < 0.001$) and *mkkk18-2* ($P < 0.0001$), respectively. Consistent with this trend for SI, the abaxial SI for *MKKK18oe* was 7% higher than for WT lines. Because GUS expression driven by the *MKKK18* promoter was detected in guard cells, we analyzed whether MKKK18 was involved in the regulation of stomatal aperture. Compared with leaves from the WT, leaves from both knockout lines showed increased stomatal aperture under normal growth conditions. However, this effect was more pronounced in the *mkkk18-2* mutant (Fig. 4B). Measurements of stomatal aperture in response to ABA revealed that stomata from the knockout lines were again significantly more open than in the WT. Accordingly, *MKKK18oe* was hypersensitive to ABA-induced stomatal closure (Fig. 4B). Next, we analyzed whether MKKK18 acted downstream of responses to $CaCl_2$ or H_2O_2 in guard-cell ABA signaling. Compared with WT Col-0, the knockout lines were significantly, if only slightly, impaired in H_2O_2-induced stomatal closure but not in response to $CaCl_2$ (Fig. 4C).

MKKK18 is activated by ABA in tobacco

To test mechanism of MKKK18 activation in response to ABA we generated a peptide-specific antibody against MKKK18. Using alignment tools, we found a unique N-terminal sequence of MKKK18 with no obvious similarity to any other *Arabidopsis* protein, including MAP kinases of any type. To test the specificity of the generated antibodies, we performed immunoprecipitation of recombinant MKKK18-GST with and without an epitope-mimicking peptide. We found that the generated antibody recognized recombinant MKKK18-GST (Fig. 5A-B), while preincubation of anti-MKKK18-coupled beads with the peptide blocked immunoprecipitation of MKKK18 (Fig. 5A). Then we tested the antibody in *Arabidopsis* extracts. We were unable to detect the MKKK18 protein directly, either by immunoblot

analysis of the total protein extract or in the immunoprecipitates from WT Col-0 and knockout lines. Nevertheless, the MKKK18 immunocomplex activity was detectable from ABA-treated WT Col-0, although not from ABA-treated knockout lines (Fig. 5C). These results clearly demonstrate the specificity of the antibody for MKKK18.

To analyse the time course of MKKK18 activation in response to ABA, we again performed the kinase immunocomplex assay using MBP as a substrate. *Nicotiana benthamiana* plants were generated that transiently expressed the *35S:MKKK18-GFP* construct, and the MKKK18-GFP protein was immunoprecipitated using the anti-MKKK18 antibody (Fig. 5D). As expected, treatment with 1 μM ABA caused an increase in the activity of MKKK18, which was observed within 60 min of treatment. Overall, our results demonstrate that MKKK18 activity is regulated by ABA.

ABI1 PP2C interacts with MKKK18 and affects its activation by ABA

Our previous results showed that MKKK18 expression was significantly affected in the *abi1td* mutant (Ludwików et al., 2009). Because MKKK18 is also ABA responsive, and ABI1 is known to be a negative regulator of ABA signaling, we then questioned whether ABI1 would affect MKKK18 function. We transformed *abi1td* protoplasts with WT and mutated forms of MKKK18 fused to GFP, and examined their subcellular localization. We observed that the distribution of the various forms of MKKK18-GFP in *abi1td* mesophyll protoplasts was similar to that in WT protoplasts, suggesting that ABI1 did not affect MKKK18 localization (Supplementary Fig. S1).

We next tested whether ABI1 would interact with MKKK18 using yeast two-hybrid, GST pull-down and BiFC assays. Full-length ABI1 (and homologous ABI2 PP2C as a control) and MKKK18 cDNA were fused to either BD or AD domains for yeast two-hybrid analysis and double-transformed yeast lines were generated. Positive results, indicating

interaction, were seen only for the ABI1-MKKK18 pair (Fig. 6A-B; Supplementary Fig. S2). The binding of ABI1 to MKKK18 was then analyzed using pull-down assays. Streptag-ABI1 (and Streptag-ABI2 as a control) purified from plant extracts were incubated with recombinant His-MKKK18 or His alone. Again, only ABI1 was capable of binding MKKK18, indicating substrate specificity of ABI1 PP2Cs for interaction with MKKK18 (Fig. 6C-D). This result was further confirmed by BiFC experiments using ABI1 (or ABI2 as a control) with MKKK18, which also revealed that ABI1 and MKKK18 were capable of interacting (Fig. 6E; Supplementary Fig. S3).

Consequently, we analyzed the effect of ABI1 PP2C activity on MKKK18 activation. *Arabidopsis* mesophyll protoplasts were transfected with *35S:MKKK18–GFP* constructs, and immunocomplex MKKK18 activity was determined by *in vitro* kinase assays in the presence of recombinant ABI1 or ABI2 proteins (Fig. 7A-B). ABI1 but not ABI2 inhibited MKKK18 kinase activity. As a control treatment, the activities of both PP2Cs were monitored with a nonradioactive phosphatase assay (Fig. 7A). Previous studies revealed that ABI1 can inhibit the autoactivation of SnRK2 kinases (Ng et al., 2011). To test the mechanism of MKKK18 activation and the role of ABI1 in this process, we purified recombinant MKKK18 and analyzed the kinase activity *in vitro* in the presence of ABI1 (and ABI2 as a negative control), the downstream substrate *in vivo* – MKK3 (Danquah et al., 2015; Matsuoka et al., 2015), an artificial substrate (MBP) and SnRK2.6 as a positive control (Fig. 7C-E). Interestingly, we observed no autophosphorylation activity of MKKK18 and in consequence no phosphorylation of the substrates, suggesting that MKKK18 activity is precisely controlled and ABI1 does not regulate autoactivation of MKKK18.

Finally, to support the role of ABI1 in the regulation of MKKK18 activity, we examined MKKK18 activation in WT Col-0 and *abi1td* after ABA treatment. Previously it is reported the MKKK18 expression is abolished in the ABA receptor quadruple *pyr1pyl1pyl2pyl4*

mutant (Danquah et al., 2015). Therefore, SnRK2.6 kinase, another crucial element of the ABA pathway, was also included in this analysis. Under the conditions indicated, we observed a stronger induction of MKKK18 activity in the *abi1td* mutant than in the WT Col-0 plants after 90 min of ABA treatment (Fig. 8A-B). At the same conditions, ABA-induced MKKK18 activation was abolished in *snrk2.6* mutant. These demonstrated that both ABI1 PP2C and SnRK2.6 affects functional activation of MKKK18 in response to ABA treatment.

Finally,

MKKK18 accumulation is regulated by ABI1 and the ubiquitin proteasome pathway

The MKKK18 protein was found to be in low abundance and, indeed, undetectable in total protein extracts from WT Col-0 plants. This feature of MKKK18 resembles other short-lived proteins, like ACC synthases 2 and 6, whose degradation is mediated by the ubiquitin proteasome pathway (Liu and Zhang, 2004; Joo et al., 2008). Recently, we demonstrated that ABI1 controls turnover of ACC synthase 6 (Ludwików et al., 2014; Ludwików, 2015); therefore, we hypothesize that ABI1 might also be involved in the regulation of MKKK18 stability. To test this hypothesis first we examined MKKK18 transcript level in WT and two independent *ABI1* knockout lines – *abi1td* (Ludwikow et al., 2009) and *abi1-2* (Saez et al. 2006). Importantly, in response to 90 min of 50 μM ABA treatment *MKKK18* expression was significantly lower in both *ABI1* knockout lines as compared to WT plants ($P < 0.0001$) (Fig. 8C). Because the decrease in MKKK18 transcript accumulation does not explain the increased MKKK18 kinase activity in the ABI1 knockout we examined the turnover of MKKK18. Cell-free degradation assays showed that recombinant GST-MKKK18 was degraded more slowly in *abi1td* than in WT cell extracts (Fig. 9A). The degradation was blocked by MG132 (a proteasome inhibitor) in both *abi1td* and WT plant extracts. The half-life of GST-MKKK18 in the assay was substantially longer in *abi1td* protein extracts

compared to WT protein extracts (Fig. 9B). Overall, these results demonstrate that ABI1 PP2C regulates MKKK18 turnover.

Importantly, slower MKKK18 degradation could result from increase protein synthesis therefore to distinguish between translational or post-translational effects we examined MKKK18 protein level in Arabidopsis protoplasts transiently expressing 35S:MKKK18-GFP treated with protein synthesis inhibitor – cycloheximide (CHX) (Fig. 9D). As expected CHX treatment significantly lowered accumulation of MAPKKK18 protein. Notably, simultaneous CHX and MG132 treatment prevents reduction of MKKK18 protein level, demonstrating that MKKK18 is degraded by proteasome pathway.

Because MAPKKK18 transcript level and kinase activity are regulated by ABA we asked whether ABA also affects the MKKK18 protein level. Again cell-free degradation assay was performed to test MKKK18 stability is affected by ABA. GST-MKKK18 recombinant protein was incubated with protein extracts prepared from the wild type treated with mock or 50 μM ABA. GST-MKKK18 was rapidly degraded when incubated with protein extracts from the WT and this degradation was blocked by ABA (Fig. 9E). These results indicate that ABA regulates MKKK18 protein stability.

DISCUSSION

Previously it was shown that ABA activates several MAP kinases to perform different functions in the cell (Danquah et al., 2014; Danquah et al., 2015). In this study, we further demonstrate that MKKK18 is an element of the ABA response pathway and that it regulates ABA signaling. We also demonstrate the specific locations for MKKK18 expression in guard cells (Fig. 1I) and in root meristem tissues (Fig. 1G). Interestingly, active MKKK18 is targeted specifically to the nucleus. We also show that MKKK18 kinase activity is increased by ABA treatment. Consistent with this, we show that MKKK18 is involved in ABA-related

responses including stomatal development (Fig. 4), stomatal movement (Fig. 4), ABA inhibition of germination and root growth (Fig. 3). Notably, we identify ABI1 PP2C as an MKKK18-interacting protein (Fig. 6) and we demonstrate that ABI1 inhibits MKKK18 activity (Fig. 7B). We also establish that MKKK18 is unstable and is degraded by the 26S proteasome, providing evidence that ABI1 promotes proteasomal degradation of MKKK18 (Fig. 9).

ABA plays a major role in various aspects of plant growth and development, and is pivotal in stomatal function (Danquah et al., 2014; Smekalova et al., 2014; Cai et al., 2014). In this study, we show that loss of MKKK18 function leads to impaired stomatal development and a constitutive phenotype with more open stomata. While both *mkkk18* knockouts showed WT sensitivity to ABA at the level of germination, the MKKK18 overexpressing lines were less sensitive, indicating that MKKK18 is required but has redundant functions in this process. A somewhat contrasting phenotype for stomatal development indicates a specific role for MKKK18 in this process. As previously documented, ABA inhibits initiation of stomatal development (Tanaka et al., 2013), reducing the number of stomata per leaf and decreasing the stomatal index (Franks and Farquhar, 2001). Consistent with this, Tanaka et al. (2013) reported that stomatal development is enhanced in ABA-insensitive mutants. Our results support this finding by showing that the stomatal index of the ABA-insensitive *MKKK18oe* lines is significantly higher than in the WT Col-0 line (Fig. 4). Accordingly, the stomatal index of both *MKKK18* knockouts are significantly lower (Fig. 4), suggesting that MKKK18 acts as a positive regulator of stomatal development. Interestingly, another MKKK, YDA, which fine-tunes this process, acts as a negative regulator in the early stages, but acts as a positive regulator in the final step of stomatal development (Wang et al., 2007; Lampard et al., 2009). Although MKKK18 and YDA likely control different pathways, they may cooperate in the final stages of stomatal development. The involvement of different MAP

cascade kinases in the same process was reviewed recently (Danquah et al., 2014), and participation of the same cascades in different processes has been reported (Wang et al., 2007; Meng et al., 2011).

As is seen from the phenotypes described in this study, *MKKK18oe* lines show different response to ABA stimulus at the level of germination versus stomata movement and root growth. The phenotypes of germinating *MKKK18oe* seedlings resulted in ABA insensitive phenotype (Fig. 3D). Overexpression of *MKKK18* causes ABA-hypersensitive stomatal closing and root growth (Fig. 3E-H), suggesting that similar MKKK18-based signaling pathways may operate in these processes. However, opposite phenotypic responses to the ABA stimulus depending on the developmental stage or particular type of cell (i.e. quad cells) indicate that MKKK18 adopts signaling system to integrate different pathways.

To determine the exact mechanism underlying MKKK18 activation, we tested the interaction between MKKK18 and the homologous phosphatases ABI1 and ABI2 (Fig. 6-7). ABI1/2 are known as negative regulators of ABA signaling that interact with the ABA receptors PYR/RCAR and SnRK2s (Park et al., 2009; Ma et al., 2009; Umezawa et al., 2009; Vlad et al., 2009). Interaction between MKKK18 and ABI1 supports the notion that the MKKK18 cascade work downstream the core ABA signalling pathway. Importantly, ABA-induced MKKK18 kinase activity is significantly increased the *ABI1* knockout while MKKK18 transcript level was significantly reduced as compared to WT. In support, the activity of MKKK18 is abolished in *snrk2.6* mutant suggesting that the components of the core ABA pathway negatively regulates MKKK18 function at multiple levels. In addition, the MKKK18 transcription was also abolished in the quadruple *pyr1pyl1pyl2pyl4* mutant (Danquah et al., 2015). Therefore, what is the role of ABI1 in regulating MKKK18 activity? Protein kinase autoactivation, via phosphorylation of the activation loop, is a common regulatory mechanism that switches the status of the signaling cascades to standby. MKKK18 does not undergo

autoactivation (Fig. 7), and therefore it must be activated by an upstream receptor kinase. Thus, ABI1 does not prevent MKKK18 autoactivation, because this does not occur, suggesting that, instead, the phosphatase is needed for down-regulation of the pathway mediated by MKKK18.

Another element of kinase activity regulation, especially in signal transduction pathways, is protein degradation via the proteasome pathway (Coulombe et al., 2003; Fragoso et al., 2009; Peng et al., 2008; Lyzenga et al., 2013; Wang and Dohlman, 2006). Ubiquitinated proteins are present in low abundance and are unstable: in mammalian cells, MEKK1 and several isoforms of extracellular signal-regulated kinases (ERKs) are degraded via the proteasome pathway, leading to inactivation of ERK1/2 and JNK pathways mediated by MEKK1 (Wang and Dohlman, 2006). In Arabidopsis, well-documented examples of protein kinase degradation include SnRK1.1, SnRK1.2, GSK3-like kinase and CIPK26 (Fragoso et al., 2009; Peng et al., 2008; Lyzenga et al., 2013). Here we demonstrate that the interaction between ABI1 and MKKK18 is necessary for the destruction of the MKKK18 kinase. As shown recently, ABI1 promotes the degradation of ACS6 protein (Ludwików et al., 20014). This new role of ABI1 phosphatase is not restricted to a single protein, but also extends to the regulation of MKKK18 activity. We show that ABI1 inhibits MKKK18 activity (Fig. 7B), and by using a cell-free assay, we reveal that ABI1 promotes its degradation (Fig. 9). These results suggest that ABI1 PP2C can be considered a key player in the ABA-dependent feedback mechanism for resetting different signaling pathways to pre-stimulatory status.

In summary, an important aspect of the current research is the identification of key regulators of the ABA response and their signaling networks. Our current findings demonstrate that phosphorylation and dephosphorylation events play an important role in the transmission of the ABA signal. Although the SnRK2 protein kinases and group A PP2C-type phosphatases constitute a core ABA signaling pathway, the involvement of other groups of

proteins, including MAP cascade kinases, has been recognized and documented in earlier studies (for the most recent review, see Danquah et al., 2014). The critical outstanding questions facing researchers are: which MAPKs are involved in ABA signal transduction, and what are the molecular details of the response to this signal? The analyses presented here demonstrate that MKKK18 is an ABA-activated kinase regulated by ABI1 and the proteasome. Based on the results presented in this study and on previously publish data (Irigoyen et al. 2014), we propose a schematic model (Fig. 10) to describe the effect of ABI1 regulation on MKKK18. Further analysis will help to elucidate novel regulatory mechanisms involving MKKK18.

METHODS

Plant growth and treatment

Arabidopsis thaliana Col-0 seeds were surface sterilized by treatment with 70% ethanol for 10 min, followed by four washes with sterile distilled water. The seeds were germinated on half-strength Murashige and Skoog (MS) medium including 1% sucrose. After a three-day stratification at 4˚C, the seeds were transferred to a growth chamber and grown as described in Ludwików et al. (2009). Seeds of *mkkk18-1* and *mkkk18-2* were obtained from the Nottingham Arabidopsis Stock Centre. The T-DNA insertion line for *abi1td* was described previously (Ludwików et al., 2009).

Plasmid construction

For protein interaction analysis in yeasts, full length ABI1 BD constructs and the PP2C catalytic domain (ΔN-ABI1) were used as described in Ludwików et al. (2009) and Ludwików et al. (2014), respectively. MKKK18 AD constructs were PCR-amplified using specific primer pairs (MKKK18fEcoRI and MKKK18rSacI), cloned into the pGEM-T Easy

vector (Promega), excised as *Eco*RI-*Sac*I restriction fragments, and ligated into the pACT2-AD vector. To generate the MKKK18 BD construct, a pUNI clone for MKKK18 (U18652) was recombined with the pACT2 vector using Cre recombinase (Liu et al., 1998). To generate the pENTR™/SD/D-TOPO® vector for facilitating the generation of C- or N-terminal in-frame MKKK18 fusions, cDNA for MKKK18 was amplified using *Pfu* polymerase, cloned into pENTR and then sequenced. To generate the recombinant GST- or His-tagged vectors, the pENTR-MKKK18 constructs were recombined with the Gateway® pDEST™15, Gateway® pDEST™17 or Gateway® pDEST™24 vectors using Gateway® LR Clonase® II Enzyme Mix (Invitrogen). For the BiFC assay, cDNAs for ABI1, ABI2 and MKKK18 were amplified using *Pfu* polymerase and then cloned into the pENTR/SD/D-TOPO vector (Invitrogen) (refer to the section "Supplementary Methods S1" for details on the construction of the BiFC vector). The clones generated were digested with *Mlu*I, and the cDNA-containing restriction fragments were recombined with the pSAT3-cCFP-DEST and the pSAT5-DEST-nVenus vectors using Gateway® LR *Clonase*® II Enzyme Mix (Invitrogen), resulting in ncECFP-ABI1/2 and cnVenus-MKKK18 constructs, respectively. The DNA construct for MKKK18 localization and plant transformation (*35S:MKKK18-GFP*) was prepared in pEarleyGate 103 (Earley et al., 2006) using Gateway technology. Two out of six independent Col-0/*35S:MKKK18-GFP* transgenic lines were tested: #1 and #2. Site-directed mutagenesis of MKKK18 was performed using a QuikChange II XL Site-Directed Mutagenesis Kit (Agilent) according to the manufacturer's protocol, and using the following oligonucleotides: K32M *For* 5'-CACTCGCCGTAATGTCCGCCGAGT-3' and *Rev* 5'-ACTCGGCGGACATTACGGCGAGTG-3'; T161E *For* 5'-GGTTGAACCGGAAATAGAGGAACCGGTTAGAGGAAC-3' and *Rev* 5'-GTTCCTCTAACCGGTTCCTCTATTTCCGGTTCAACC-3'.

Construction of the *MKKK18* promoter-GUS vector

The 1622 bp *MKKK18* promoter region was generated from genomic *Arabidopsis* DNA by PCR amplification using different primers (Supplementary Table S1). The promoter sequence was verified by sequencing. BLAST analysis confirmed that isolated fragments had 99% identity with the known *MKKK18* promoter region deposited in the TAIR database. To produce the 1622 bp *MKKK18* promoter region (the *D::GUS* construct) the PCR products were cloned into pGEM T-Easy vector system (Promega), sequenced and cloned into the *KpnI-PstI* sites of the pBI101 vector. The Promoter-reporter fusion construct was transformed into *Agrobacterium tumefaciens* strain LBA4404 and used for *Arabidopsis thaliana* (Columbia, Col-0) plant transformations using the floral dip method (Clough et al., 1998). More than five independent transgenic lines were produced and tested for responsiveness by GUS histochemical assays. Three representative lines were selected for detailed characterization and showed the same expression pattern for all of the tested conditions.

Histochemical localization of GUS expression

For histochemical analysis of *GUS* expression, T2 seeds of Col-0/*ProMKKK18*:*GUS* were grown as described and exposed to 1 μM ABA for 24 h. Tissue samples were immersed in staining buffer [100 mM sodium phosphate, pH 7.0, 10 mM EDTA, 0.5 mM $K_4Fe(CN)_6$, 0.5 mM $K_3Fe(CN)_6$, 0.1% Triton X-100, and 1 mM X-gluc], and incubated overnight at 37˚C. After the GUS reaction, plant samples were incubated in 80% ethanol to remove chlorophyll from the green tissues. GUS staining patterns were recorded using a Zeiss Stereo Lumar V12 microscope.

Analyses of the *mkkk18-1* and *mkkk18-2* T-DNA insertion lines

The *mkkk18-1* and the *mkkk18-2* T-DNA insertion lines were isolated from SALK insertion lines (SALK_087047) and from the GABI-Kat collection (GK-244G02), respectively. The qPCR analyses were performed as described in Ludwików et al. (2009).

Stomatal index and stomatal aperture

The stomatal index (SI) was calculated based on the method described in Tanaka et al. (2013). Counts of stomata and pavement cells were performed on five areas of each cotyledon from 10 separate seedlings, giving 100 measurements per experiment, using a Nikon Eclipse Ti microscope with a Nikon Digital Sight DS-Fi1c camera. The SI was calculated individually for each cotyledon using the formula: SI = [number of stomata / (number of other epidermal cells + number of stomata)]. For statistical analysis, Student's *t*-test was performed. For guard-cell aperture measurements, rosette leaves of 5-week-old plants were floated in opening buffer (10 mM KCl, 7.5 mM EGTA, 10 mM Mes-KOH, at pH 6.15) and incubated at 20°C under light conditions for 2 h to open the stomata. Subsequently, the same opening buffer was supplemented with either 15 μM ABA or 1 mM H_2O_2 or 1 mM $CaCl_2$, and the leaves were incubated for another 2 h. The stomatal apertures (width divided by length) along three different epidermal transects were measured using a Nikon Eclipse Ti (with Nikon Digital Sight DS-Fi1c digital camera) and Nikon NIS Elements AR software. No less than 60 mature stomata were analyzed per transect.

Protoplast isolation, transformation and transient expression assays

Transient expression assays were performed using protoplasts from Arabidopsis mesophyll cells. Protoplast isolation, transformation, and transient expression assays were performed based on methods described in Ludwików et al. (2014). Protoplasts were transiently transformed with 5 µg plasmid, collected by centrifugation and resuspended in lysis buffer for

further analysis. Transient protein expression in tobacco leaves was performed as described in Voinnet et al. (2003). *Agrobacterium tumefaciens* C58C1 cells with different MKKK18 constructs were mixed with an equal volume of *Agrobacterium* C58C1 (*pCH32 35S:p19*) expressing the silencing suppressor p19. The bacteria were injected into fully expanded leaves of tobacco plants, and were examined after five days.

Kinase activity assays

For the *in vitro* kinase assays, the MKKK18 immunocomplex assay was performed based on methods described in Ludwików et al. (2014). Briefly, tissue extracts containing 500 μg total protein were immunoprecipitated for 1 h at 4˚C with 5 μg anti-GFP or anti-MKKK18 antibody pre-coupled to Dynabeads Protein-A (Invitrogen). This mixture was washed three times with wash buffer I (20 mM Tris-HCl, 5 mM EDTA, 100 mM NaCl, 1% Triton X-100), once with the same buffer but containing 1 M NaCl, and once with kinase buffer (20 mM Hepes, pH 7.5, 10 mM $MgCl_2$, 1 mM DTT). A half-aliquot of MKKK18 was used to phosphorylate 5 μg of substrate, (myelin basic protein – MBP; Sigma), in kinase buffer containing 25 μM ATP and [γ-^{32}P]ATP (2 μCi per reaction) at 30˚C. Another half-aliquot of activated MKKK18 was assayed under the same conditions without radioactive ATP. The reactions were stopped by the addition of SDS-loading buffer after 60 min. SDS-PAGE reaction products were analyzed using autoradiography or Western blotting.

Immunoblotting

Proteins were separated on a 10% SDS-PAGE gel (BioRad) and were transferred onto Immobilon-P membranes (Millipore). The membranes were blocked for 1 h in PBS-T containing a 3% blocking solution, washed three times, and incubated for 1 h with rabbit anti-GFP (1:200; sc-8334, Santa Cruz Biotechnology), StrepMAB-Classic (1:3000; IBA

BioTAGnology), anti-GST-Tag (1:5000; Sigma), and anti MKKK18 antibody (AS13 2673, Agrisera). After washing three times, the membranes were incubated for 1 h with the appropriate secondary antibody. Detection was performed with ECL (Thermo Scientific) according to the manufacturer's instructions.

GST-tagged protein overexpression, purification, pull-down and cell-free degradation assays

Escherichia coli BL21(DE3) competent cells were transformed with recombinant MKKK18-GST, GST-ABI1 and GST-ABI2 expression constructs. Bacterial growth, isolation of recombinant GST-fusion proteins, pull-down assays and cell-free degradation assays were conducted according to Ludwików et al. (2014). The abundance of MKKK18-GST was determined using anti-GST antibodies.

Bimolecular fluorescence complementation (BIFC) in *Arabidopsis* protoplasts

For the BiFC analysis, various combinations of plasmids encoding cECFP, nVenus fusion proteins and RFP proteins as an internal control were mixed at a 1:1:1 (w/w) ratio, and the mixture of plasmid DNA was used for PEG-mediated transformation as described by Ludwików et al. (2014).

FUNDING

This work was supported by "Grants for Interdisciplinary Grants" from the Dean of the Faculty of Biology (No. GIWB-02/2011), by a Grant from the National Science Centre (No. DEC-2012/05/B/NZ3/00352) to AL and (No. DEC-2011/03/N/NZ3/01796) to MM.

AKNOWLEDGEMENT

We thank David Baulcombe for providing the p19 vector construct and *Agrobacterium* C58C1 strain and Hanna Korcz-Szatkowska for excellent technical assistance.

REFERENCES

Bate, N., and Twell, D. (1998) Functional architecture of a late pollen promoter: pollen-specific transcription is developmentally regulated by multiple stage-specific and co-dependent activator elements. *Plant Mol. Biol.* 37: 859-869.

Boudsocq, M., Willmann, M.R., McCormack, M., Lee, H., Shan, L., He, P., Bush, J., Cheng, S.H., and Sheen, J. (2010) Differential innate immune signaling via Ca(2+) sensor protein kinases. *Nature.* 464: 418-422.

Brock, A.K., Willmann, R., Kolb, D., Grefen, L., Lajunen, H.M., Bethke, G., Lee, J., Nurnberger, T., and Gust, A.A. (2010) The Arabidopsis mitogen-activated protein kinase phosphatase PP2C5 affects seed germination, stomatal aperture, and abscisic acid-inducible gene expression. *Plant Physiol.* 153: 1098-1111.

Cai, G., Wang, G., Wang, L., Pan, J., Liu, Y., and Li, D. (2014) ZmMKK1, a novel group A mitogen-activated protein kinase kinase gene in maize, conferred chilling stress tolerance and was involved in pathogen defense in transgenic tobacco. *Plant Science.* 214: 57-73.

Clough, S.J., and Bent, A.F. (1998) Floral dip: a simplified method for *Agrobacterium*-mediated transformation of *Arabidopsis thaliana*. *Plant J.* 16: 735–743.

Colcombet, J., and Hirt, H. (2008) Arabidopsis MAPKs: a complex signaling network involved in multiple biological processes. *Biochem. J.* 413: 217-226.

Coulombe, P., Rodier, G., Pelletier, S., Pellerin, J., and Meloche, S. (2003) Rapid turnover of extracellular signal-regulated kinase 3 by the ubiquitin-proteasome pathway defines a novel paradigm of mitogen-activated protein kinase regulation during cellular differentiation. *Mol. Cell Biol*. 23: 4542-4558.

Danquah, A., de, Z.A., Colcombet, J., and Hirt, H. (2014) The role of ABA and MAPK signaling pathways in plant abiotic stress responses. *Biotechnol. Adv.* 32: 40-52.

Danquah, A., de Zélicourt, A., Boudsocq, M., Neubauer, J., Frei dit Frey, N., Leonhardt, N., Pateyron, S., Gwinner, F., Tamby, J.-P., Ortiz-Masia, D., Marcote, M. J., Hirt, H. and Colcombet, J. (2015), Identification and characterization of an ABA-activated MAP kinase cascade in *Arabidopsis thaliana*. *Plant J.,* 82: 232–244.

de Torres-Zabala, M., Truman, W., Bennett, M.H., Lafforgue, G., Mansfield, J.W., Rodriguez, E.P., Bogre, L., and Grant, M. (2007) Pseudomonas syringae pv. tomato hijacks the Arabidopsis abscisic acid signaling pathway to cause disease. *EMBO J.* 26: 1434-1443.

Dupeux, F., Santiago, J., Betz, K., Twycross, J., Park, S.Y., Rodriguez, L., Gonzalez-Guzman, M., Jensen, M.R., Krasnogor, N., Blackledge, M., Holdsworth, M., Cutler, S.R., Rodriguez, P.L., and Marquez, J.A. (2011) A thermodynamic switch modulates abscisic acid receptor sensitivity. *EMBO J.* 30: 4171-4184.

Dupeux, F., Antoni, R., Betz, K., Santiago, J., Gonzalez-Guzman, M., Rodriguez, L., Rubio, S., Park, S.Y., Cutler, S.R., Rodriguez, P.L., and Marquez, J.A. (2011) Modulation of abscisic acid signaling in vivo by an engineered receptor-insensitive protein phosphatase type 2C allele. *Plant Physiol.* 156: 106-116.

Earley, K.W., Haag, J.R., Pontes, O., Opper, K., Juehne, T., Song, K., and Pikaard, C.S. (2006) Gateway-compatible vectors for plant functional genomics and proteomics. *Plant J.* 45: 616-629.

Fragoso, S., Espindola, L., Paez-Valencia, J., Gamboa, A., Camacho, Y., Martinez-Barajas, E., and Coello, P. (2009) SnRK1 isoforms AKIN10 and AKIN11 are differentially regulated in Arabidopsis plants under phosphate starvation. *Plant Physiol.* 149: 1906-1916.

Franks, P.J., and Farquhar, G.D. (2001) The effect of exogenous abscisic acid on stomatal development, stomatal mechanics, and leaf gas exchange in *Tradescantia virginiana*. *Plant Physiol.* 125: 935-942.

Fujita, Y., Nakashima, K., Yoshida, T., Katagiri, T., Kidokoro, S., Kanamori, N., Umezawa, T., Fujita, M., Maruyama, K., Ishiyama, K., Kobayashi, M., Nakasone, S., Yamada, K., Ito, T., Shinozaki, K., and Yamaguchi-Shinozaki, K. (2009) Three SnRK2 protein kinases are the main positive regulators of abscisic acid signaling in response to water stress in Arabidopsis. *Plant Cell Physiol.* 50: 2123-2132.

Geiger, D., Scherzer, S., Mumm, P., Stange, A., Marten, I., Bauer, H., Ache, P., Matschi, S., Liese, A., Al-Rasheid, K.A., Romeis, T., and Hedrich, R. (2009) Activity of guard cell anion channel SLAC1 is controlled by drought-stress signaling kinase-phosphatase pair. *Proc.* Natl Acad. *Sci. USA.* 106: 21425-21430.

Guo, Y., Xiong, L., Song, C.P., Gong, D., Halfter, U., and Zhu, J.K. (2002) A calcium sensor and its interacting protein kinase are global regulators of abscisic acid signaling in Arabidopsis. *Dev. Cell.* 3: 233-244.

Himmelbach A., Hoffmann T., Leube M., Hohener B., and Grill E. (2002) Homeodomain protein ATHB6 is a target of the protein phosphatase ABI1 and regulates hormone responses in Arabidopsis. *EMBO J.* 21: 3029-3038.

Hoth, S., Morgante, M., Sanchez, J.P., Hanafey, M.K., Tingey, S.V., and Chua, N.H. (2002) Genome-wide gene expression profiling in Arabidopsis thaliana reveals new targets of abscisic acid and largely impaired gene regulation in the *abi1-1* mutant. *J. Cell Sci.* 115: 4891-4900.

Irigoyen, M.L., Iniesto, E., Rodriguez, L., Puga, M.I., Yanagawa, Y., Pick, E., Strickland, E., Paz-Ares, J., Wei, N., Jaeger, G., Rodriguez, P.L., Deng, X.W., and Rubio, V. (2014) Targeted Degradation of Abscisic Acid Receptors Is Mediated by the Ubiquitin Ligase Substrate Adaptor DDA1 in Arabidopsis. *Plant Cell.* 10.1105/tpc.113.122234.

Jammes F., Song C., Shin D., Munemasa S., Takeda K., Gu D., Cho D., Lee S., Giordo R., Sritubtim S., Leonhardt N., Ellis B.E., Murata Y., and Kwak, J.M. (2009) MAP kinases MPK9 and MPK12 are preferentially expressed in guard cells and positively regulate ROS-mediated ABA signaling. *Proc. Natl Acad. Sci. USA.* 106: 20520-20525.

Jammes, F., Yang, X., Xiao, S., and Kwak, J.M. (2011) Two Arabidopsis guard cell-preferential MAPK genes, MPK9 and MPK12, function in biotic stress response. *Plant Signal. Behav.* 6: 1875-1877.

Jonak, C., Okrész, L., Bögre, L., and Hirt, H. (2002) Complexity, cross talk and integration of plant MAP kinase signalling. *Curr Opin Plant Biol.* 5: 415-424.

Joo, S., Liu, Y., Lueth, A., and Zhang, S. (2008) MAPK phosphorylation-induced stabilization of ACS6 protein is mediated by the non-catalytic C-terminal domain, which also contains the cis-determinant for rapid degradation by the 26S proteasome pathway. *Plant J.* 54: 129-140.

Kong, Q., Qu, N., Gao, M., Zhang, Z., Ding, X., Yang, F., Li, Y., Dong, O.X., Chen, S., Li, X., and Zhang, Y. (2012) The MEKK1-MKK1/MKK2-MPK4 kinase cascade negatively regulates immunity mediated by a mitogen-activated protein kinase kinase kinase in Arabidopsis. *Plant Cell.* 24: 2225-2236.

Krawczyk, S., Thurow, C., Niggeweg, R., and Gatz, C. (2002) Analysis of the spacing between the two palindromes of activation sequence-1 with respect to binding to different TGA factors and transcriptional activation potential. *Nucl. Acids Res.* 30: 775-781.

Lampard, G.R., Lukowitz, W., Ellis, B.E., and Bergmann, D.C. (2009) Novel and expanded roles for MAPK signaling in Arabidopsis stomatal cell fate revealed by cell type-specific manipulations. *Plant Cell.* 21: 3506-3517.

Leung, J., Orfanidi, S., Chefdor, F., Meszaros,, T., Bolte, S., Mizoguchi, T., Shinozaki, K., Giraudat, J., and Bogre, L. (2006) Antagonistic interaction between MAP kinase and protein phosphatase 2C in stress recovery. *Plant Science.* 171: 596–606.

Leonhardt, N., Kwak, J.M., Robert, N., Waner, D., Leonhardt, G., and Schroeder, J.I. (2004) Microarray expression analyses of Arabidopsis guard cells and isolation of a recessive abscisic acid hypersensitive protein phosphatase 2C mutant. *Plant Cell.* 16: 596-615.

Liu, Q., Li, M.Z., Leibham, D., Cortez, D., and Elledge, S.J. (1998) The univector plasmid-fusion system, a method for rapid construction of recombinant DNA without restriction enzymes. *Current Biol.* 8: 1300-1309.

Liu, Y., and Zhang, S. (2004) Phosphorylation of 1-aminocyclopropane-1-carboxylic acid synthase by MPK6, a stress-responsive mitogen-activated protein kinase, induces ethylene biosynthesis in Arabidopsis. *Plant Cell.* 16: 3386-3399.

Ludwikow, A., Kierzek, D., Gallois, P., Zeef, L., and Sadowski, J. (2009) Gene expression profiling of ozone-treated Arabidopsis *abi1td* insertional mutant: protein phosphatase 2C ABI1 modulates biosynthesis ratio of ABA and ethylene. *Planta.* 230: 1003-1017.

Ludwików, A., Babula-Skowrońska, D., Szczepaniak, M., Belter, N., Dominiak, E. and Sadowski, J. (2013) Expression profiles and genomic organisation of group A protein phosphatase 2C genes in *Brassica oleracea*. *Ann Appl Biol*. 163: 124-134.

Ludwikow, A., Ciesla, A., Kasprowicz-Maluski, A., Mitula, F., Tajdel, M., Galganski, L., Ziolkowski, P.A., Kubiak, P., Malecka, A., Piechalak, A., Szabat, M., Gorska, A., Dabrowski, M., Ibragimow, I., and Sadowski, J. (2014) Arabidopsis Protein Phosphatase 2C ABI1 Interacts with Type I ACC Synthases and Is Involved in the Regulation of Ozone-Induced Ethylene Biosynthesis. *Mol. Plant.* 7: 960-976.

Ludwików A (2015) Targeting proteins for proteasomal degradation—a new function of Arabidopsis ABI1 protein phosphatase 2C. *Front. Plant Sci.* 6: 310.

Lyzenga, W.J., Liu, H., Schofield, A., Muise-Hennessey, A., and Stone, S.L. (2013) Arabidopsis CIPK26 interacts with KEG, components of the ABA signaling network and is degraded by the ubiquitin-proteasome system. *J. Exp. Bot.* 64: 2779-2791.

Ma, Y., Szostkiewicz, I., Korte, A., Moes, D., Yang, Y., Christmann, A., and Grill, E. (2009) Regulators of PP2C phosphatase activity function as abscisic acid sensors. *Science.* 324: 1064-1068.

Mane, S.P., Vasquez-Robinet, C., Sioson, A.A., Heath, L.S., and Grene, R. (2007) Early PLDalpha-mediated events in response to progressive drought stress in Arabidopsis: a transcriptome analysis. *J. Exp. Bot.* 58: 241-252.

Matsuoka, D., Yasufuku, T., Furuya, T., and Nanmori, T. (2015) An abscisic acid inducible Arabidopsis MAPKKK, MAPKKK18 regulates leaf senescence via its kinase activity. *Plant Mol Biol.* 87: 565-575.

Meng, X., Wang, H., He, Y., Liu, Y., Walker, J.C., Torii, K.U., and Zhang, S. (2012) A MAPK cascade downstream of ERECTA receptor-like protein kinase regulates Arabidopsis inflorescence architecture by promoting localized cell proliferation. *Plant Cell.* 24: 4948-4960.

Miao, Y., Lv, D., Wang, P., Wang, X.C., Chen, J., Miao, C., and Song, C.P. (2006) An Arabidopsis glutathione peroxidase functions as both a redox transducer and a scavenger in abscisic acid and drought stress responses. *Plant Cell.* 18: 2749-2766.

Nakashima, K., Fujita, Y., Kanamori, N., Katagiri, T., Umezawa, T., Kidokoro, S., Maruyama, K., Yoshida, T., Ishiyama, K., Kobayashi, M., Shinozaki, K., and Yamaguchi-Shinozaki, K. (2009) Three Arabidopsis SnRK2 protein kinases, SRK2D/SnRK2.2, SRK2E/SnRK2.6/OST1 and SRK2I/SnRK2.3, involved in ABA signaling are essential for the control of seed development and dormancy. *Plant Cell Physiol.* 50: 1345-1363.

Ng, L.M., Soon, F.F., Zhou, X.E., West, G.M., Kovach, A., Suino-Powell, K.M., Chalmers, M.J., Li, J., Yong, E.L., Zhu, J.K., Griffin, P.R., Melcher, K., and Xu, H.E. (2011) Structural basis for basal activity and autoactivation of abscisic acid (ABA) signaling SnRK2 kinases. *Proc. Natl Acad. Sci. USA.* 108: 21259-21264.

Nicaise, V., Roux, M., and Zipfel, C. (2009) Recent advances in PAMP-triggered immunity against bacteria: pattern recognition receptors watch over and raise the alarm. *Plant Physiol.* 150: 1638-1647.

Nishimura, N., Hitomi, K., Arvai, A.S., Rambo, R.P., Hitomi, C., Cutler, S.R., Schroeder, J.I., and Getzoff, E.D. (2009) Structural mechanism of abscisic acid binding and signaling by dimeric PYR1. *Science.* 326: 1373-1379.

Nishimura, N., Sarkeshik, A., Nito, K., Park, S.Y., Wang, A., Carvalho, P.C., Lee, S., Caddell, D.F., Cutler, S.R., Chory, J., Yates, J.R., and Schroeder, J.I. (2010) PYR/PYL/RCAR family members are major in-vivo ABI1 protein phosphatase 2C-interacting proteins in Arabidopsis. *Plant J.* 61: 290-299.

Ohta, M., Guo, Y., Halfter, U., and Zhu, J.K. (2003) A novel domain in the protein kinase SOS2 mediates interaction with the protein phosphatase 2C ABI2. *Proc.* Natl Acad. *Sci. USA*. 100: 11771-11776.

Okamoto, M., Peterson, F.C., Defries, A., Park, S.Y., Endo, A., Nambara, E., Volkman, B.F., and Cutler, S.R. (2013) Activation of dimeric ABA receptors elicits guard cell closure, ABA-regulated gene expression, and drought tolerance. *Proc.* Natl Acad. *Sci. USA*. 110: 12132-12137.

Park, S.Y., Fung, P., Nishimura, N., Jensen, D.R., Fujii, H., Zhao, Y., Lumba, S., Santiago, J., Rodrigues, A., Chow, T.F., Alfred, S.E., Bonetta, D., Finkelstein, R., Provart, N.J., Desveaux, D., Rodriguez, P.L., McCourt, P., Zhu, J.K., Schroeder, J.I., Volkman, B.F., and Cutler, S.R. (2009) Abscisic acid inhibits type 2C protein phosphatases via the PYR/PYL family of START proteins. *Science.* 324: 1068-1071.

Peng, P., Yan, Z., Zhu, Y., and Li, J. (2008) Regulation of the Arabidopsis GSK3-like Kinase BRASSINOSTEROID-INSENSITIVE 2 through Proteasome-Mediated Protein Degradation. *Mol. Plant.* 1: 338-346.

Pitzschke, A., Djamei, A., Bitton, F., and Hirt, H. (2009) A major role of the MEKK1-MKK1/2-MPK4 pathway in ROS signaling. *Mol. Plant.* 2: 120-137.

Plesch, G., Ehrhardt, T., and Mueller-Roeber, B. (2001) Involvement of TAAAG elements suggests a role for Dof transcription factors in guard cell-specific gene expression. *Plant J.* 28: 455-464.

Qiu, J.L., Zhou, L., Yun, B.W., Nielsen, H.B., Fiil, B.K., Petersen, K., Mackinlay, J., Loake, G.J., Mundy, J., and Morris, P.C. (2008) Arabidopsis mitogen-activated protein kinase kinases MKK1 and MKK2 have overlapping functions in defense signaling mediated by MEKK1, MPK4, and MKS1. *Plant Physiol.* 148: 212-222.

Saez, A., Rodrigues, A., Santiago, J., Rubio, S., and Rodriguez, P.L. (2008) HAB1-SWI3B interaction reveals a link between abscisic acid signaling and putative SWI/SNF chromatin-remodeling complexes in Arabidopsis. *Plant Cell.* 20: 2972-2988.

Salam, M.A., Jammes, F., Hossain, M.A., Ye, W., Nakamura, Y., Mori, I.C., Kwak, J.M., and Murata, Y. (2013) Two guard cell-preferential MAPKs, MPK9 and MPK12, regulate YEL signaling in Arabidopsis guard cells. *Plant Biol. (Stuttg).* 15: 436-442.

Santiago, J., Dupeux, F., Round, A., Antoni, R., Park, S.Y., Jamin, M., Cutler, S.R., Rodriguez, P.L., and Marquez, J.A. (2009) The abscisic acid receptor PYR1 in complex with abscisic acid. *Nature.* 462: 665-668.

Smekalova, V., Luptovciak, I., Komis, G., Samajova, O., Ovecka, M., Doskocilova, A., Takac, T., Vadovic, P., Novak, O., Pechan, T., Ziemann, A., Kosutova, P., and Samaj, J. (2014) Involvement of YODA and mitogen activated protein kinase 6 in Arabidopsis post-embryogenic root development through auxin up-regulation and cell division plane orientation. *New Phytol.* doi: 10.1111/nph.12880.

Suarez-Rodriguez, M.C., Adams-Phillips, L., Liu, Y., Wang, H., Su, S.H., Jester, P.J., Zhang, S., Bent, A.F., and Krysan, P.J. (2007) MEKK1 is required for flg22-induced MPK4 activation in Arabidopsis plants. *Plant Physiol.* 143: 661-669.

Szostkiewicz, I., Richter, K., Kepka, M., Demmel, S., Ma, Y., Korte, A., Assaad, F.F., Christmann, A., and Grill, E. (2010) Closely related receptor complexes differ in their ABA selectivity and sensitivity. *Plant J.* 61: 25-35.

Takeuchi, J., Okamoto, M., Akiyama, T., Muto, T., Yajima, S., Sue, M., Seo, M., Kanno, Y., Kamo, T., Endo, A., Nambara, E., Hirai, N., Ohnishi, T., Cutler, S.R., and Todoroki, Y. (2014) Designed abscisic acid analogs as antagonists of PYL-PP2C receptor interactions. *Nat. Chem. Biol.* 10: 477-482.

Taki, N., Sasaki-Sekimoto, Y., Obayashi, T., Kikuta, A., Kobayashi, K., Ainai, T., Yagi, K., Sakurai, N., Suzuki, H., Masuda, T., Takamiya, K., Shibata, D., Kobayashi, Y., and Ohta, H. (2005) 12-oxo-phytodienoic acid triggers expression of a distinct set of genes and plays a role in wound-induced gene expression in Arabidopsis. *Plant Physiol.* 139: 1268-1283.

Tanaka, Y., Nose, T., Jikumaru, Y., and Kamiya, Y. (2013) ABA inhibits entry into stomatal-lineage development in Arabidopsis leaves. *Plant J.* 74: 448-457.

Umezawa, T., Sugiyama, N., Mizoguchi, M., Hayashi, S., Myouga, F., Yamaguchi-Shinozaki, K., Ishihama, Y., Hirayama, T., and Shinozaki, K. (2009) Type 2C protein phosphatases directly regulate abscisic acid-activated protein kinases in Arabidopsis. *Proc.* Natl. Acad. *Sci. USA*. 106: 17588-17593.

Vlad, F., Rubio, S., Rodrigues, A., Sirichandra, C., Belin, C., Robert, N., Leung, J., Rodriguez, P.L., Lauriere, C., and Merlot, S. (2009) Protein phosphatases 2C regulate the activation of the Snf1-related kinase OST1 by abscisic acid in Arabidopsis. *Plant Cell.* 21: 3170-3184.

Voinnet, O., Rivas, S., Mestre, P., and Baulcombe, D. (2003) An enhanced transient expression system in plants based on suppression of gene silencing by the p19 protein of tomato bushy stunt virus. *Plant J.* 33: 949-956.

Wang, H., Ngwenyama, N., Liu, Y., Walker, J.C., and Zhang, S. (2007) Stomatal development and patterning are regulated by environmentally responsive mitogen-activated protein kinases in Arabidopsis. *Plant Cell.* 19: 63-73.

Wang, X.J., Zhu, S.Y., Lu, Y.F., Zhao, R., Xin, Q., Wang, X.F., and Zhang, D.P. (2010) Two coupled components of the mitogen-activated protein kinase cascade MdMPK1 and MdMKK1 from apple function in ABA signal transduction. *Plant Cell Physiol.* 51: 754-766.

Wang, Y., and Dohlman, H.G. (2006) Regulation of G protein and mitogen-activated protein kinase signaling by ubiquitination: insights from model organisms. *Circ. Res.* 99: 1305-1314.

Xing, Y., Jia, W., and Zhang, J. (2008) AtMKK1 mediates ABA-induced CAT1 expression and H2O2 production via AtMPK6-coupled signaling in Arabidopsis. *Plant J.* 54: 440-451.

Xiong, L., Lee, H., Ishitani, M., and Zhu, J.K. (2002) Regulation of osmotic stress-responsive gene expression by the LOS6/ABA1 locus in Arabidopsis. *J. Biol. Chem.* 277: 8588-8596.

Yamaguchi-Shinozaki, K, and Shinozaki, K. (2005) Organization of cis-acting regulatory elements in osmotic- and cold-stress-responsive promoters. *Trends Plant Sci.* 10: 88-94.

Yamasaki, K., Kigawa, T., Watanabe, S., Inoue, M., Yamasaki, T., Seki, M., Shinozaki, K., and Yokoyama, S. (2012) Structural basis for sequence-specific DNA recognition by an Arabidopsis WRKY transcription factor. *J. Biol. Chem.* 287: 7683-7691.

Yoon, J.H., Choi, E.J., and Parker, R. (2010) Dcp2 phosphorylation by Ste20 modulates stress granule assembly and mRNA decay in *Saccharomyces cerevisiae*. *J. Cell Biol.* 189: 813–827.

Yoshida, T., Fujita, Y., Sayama, H., Kidokoro, S., Maruyama, K., Mizoi, J., Shinozaki, K., and Yamaguchi-Shinozaki, K. (2010) AREB1, AREB2, and ABF3 are master transcription factors that cooperatively regulate ABRE-dependent ABA signaling involved in drought stress tolerance and require ABA for full activation. *Plant J.* 61: 672-685.

Zhu, S.Y., Yu, X.C., Wang, X.J., Zhao, R., Li, Y., Fan, R.C., Shang, Y., Du, S.Y., Wang, X.F., Wu, F.Q., Xu, Y.H., Zhang, X.Y., and Zhang, D.P. (2007) Two calcium-dependent protein kinases, CPK4 and CPK11, regulate abscisic acid signal transduction in Arabidopsis. *Plant Cell.* 19: 3019-3036.

FIGURE LEGENDS

Figure 1. Analysis of the activity of the *MKKK18* promoter in transgenic plants expressing the *Pro::MKKK18-GUS* construct

A. Schematic map of the MKKK18 promoter used for transformation and tissue-specific expression of *MKKK18*. **B.** The Pro*MKKK18*:*GUS* seedlings were germinated and grown on half-strength MS media. Five-week-old plants were treated with either 0.1% methanol (mock) or 100 μM ABA. One representative of five independent lines is shown. (A). No changes in GUS activity after the mock treatment. The bar represents 2000 μm. (B–J). Plant samples 24 h after ABA treatment. GUS activity is visible in rosette leaves (B), flower buds and sepals (C), meristem tissues (D), pistils (E), anther filaments (F), lateral roots (G), trichomes (H), leaf guard cells (I), and hydathodes (J).

Figure 2. Subcellular localization of the MKKK18 protein in *Arabidopsis* protoplasts

Active MKKK18 is localized in the nucleus. **A.** Microscopy images show nuclear localization of the MKKK18-GFP fusions in *Arabidopsis* protoplasts. Hoechst H33342 was used as

nuclear localization marker. Scale bars are calibrated to 50 μm. **B.** MKKK18 protein expression and activity were analyzed by immunoprecipitation using protein specific anti-MKKK18 antibodies and immunocomplex kinase assay with MBP as a substrate. The immunocomplex assay confirmed residual kinase activity of the *MKKK18*K32M-*GFP* allele. Western blot detection using anti-GFP antibodies corroborates the presence of MKKK18-GFP fusion proteins. CBB staining confirmed equal loading.

Figure 3. Germination and root growth assays

A–B. T-DNA insertion sites derived from the sequencing of genomic DNA isolated from *mkkk18-1* and *mkkk18-2* mutant lines. Black boxes represent an ORF. Homozygous knockout mutants were verified by PCR-based genotyping using the following primers: MKKK18LP, MKKK18RP and LBb1 for *mkkk18-1* analysis; MEK18F and GKatTDNA for *mkkk18-2* genotyping. Primer sequences are indicated in Supplementary Table S1. **C.** qPCR analysis confirmed a lack of *MKKK18* expression in homozygous lines. Each quantification was repeated twice with similar results. The results are $\log_2$ relative *MKKK18/18S* rDNA expression ratio, ± SE (n = 6). **D.** The RD29B and *RAB18* transcript levels in MKKK18 mutants. RD29B and *RAB18* expression levels were determined using three biological replicates and were normalized against 18S rDNA. Each quantification was repeated twice on separate plates. The results are displayed as mean Log2 fold change ± SE (n = 9) of three independent experiments with consistent results. **E-F.** Germination and root growth assays. ABA-mediated inhibition of germination (E) and primary root growth (F) in WT Col-0, *MKKK18oe* and *MKKK18* knockout lines. Both *MKKK18oe* #1 and #2 lines showed similar results. Values are mean ± SE for three independent experiments. Data are means and standard errors (n = 30). The asterisk indicates $P < 0.01$ (*), $P < 0.001$ (**), and $P < 0.0001$ (***) with respect to control WT Col-0 line.

Figure 4. Stomatal development and movements in *MKKK18* knockouts and the *MKKK18*-overexpressing line

A. Stomatal development is enhanced in the *MKKK18* overexpressing lines. Representative line drawings show the abaxial surface of cotyledons at day 10. Change in stomatal index and the number of guard cells (GC) and pavement cells (PC) per cotyledon in WT Col-0, *MKKK18oe*, and MKKK18 knockouts. Data represent mean ± SD (n = 300) of three independent experiments. Scale bar = 50 μm. **B.** Increased stomatal aperture of *mkkk18-1* and *mkkk18-2* knockouts compared to the WT in standard conditions (three independent experiments, 60-80 stomatal apertures at each data point). **C.** The *mkkk18-1* and *mkkk18-2* knockouts are insensitive to ABA- and H_2O_2-induced stomatal closing (two independent experiments, 80 stomatal apertures at each data point). *MKKK18oe* lines were hypersensitive to ABA-, $CaCl_2$-, and H_2O_2-induced stomatal closure (two independent experiments, 100 stomatal apertures at each data point).

Figure 5. ABA induces rapid MKKK18 activation in tobacco

A–C. Generation of MKKK18-specific antibodies. **A**. MKKK18 peptide competition assay. Recombinant GST-MKKK18 protein was incubated with anti-MKKK18 with and without 45 μg of blocking peptide. A single band of ~ 65 kDa specific to GST-MKKK18 is absent in the immunoprecipitates containing the blocking peptide. Immunodetection was performed using anti-MKKK18 antibody. **B**. MKKK18-GFP protein immunoprecipitated from tobacco total protein extracts using anti-MKKK18 and anti-GFP antibodies. Immunoblotting with anti-GFP antibodies confirmed the presence of MKKK18-GFP fusion protein. Arrows/Ab indicate excess anti-MKKK18 antibody. **C.** Analysis of MKKK18 activity in the *mkkk18* knockouts lines. MKKK18 protein was immunoprecipitated from 600 μg of total protein extracts

isolated from ABA-treated WT Col-0, *mkkk18-1*, *mkkk18-2*, and *MKKK18oe* using specific anti-MKKK18 antibodies. Immunocomplex activity was performed using MBP (2 μg) as a substrate. CBB staining of MBP confirmed equal loading**. D.** Tobacco plants infiltrated with *Agrobacterium* strain C58C1 harboring *35S:MKKK18-GFP* and *35S:p19* constructs for transient expression. Four to five days after infiltration, the tobacco plants were treated with ABA and tissue samples were collected at the indicated time points. MKKK18 activity was assessed by the immunocomplex assay using anti-MKKK18 antibody and MBP as a substrate. MKKK18-GFP was detected with anti-GFP antibody. CBB staining of MBP confirmed equal loading. The above experiments were repeated several times with similar results.

Figure 6. MKKK18 interacts with the ABI1 protein phosphatase

A. Yeast two-hybrid analysis of the interaction between MKKK18 and ABI1/2 PP2Cs. Diploid yeast colonies were grown on double (DDO-SD medium without Leu and Trp) or quadruple selective medium (QDO-SD medium without Leu, Trp, His, or Ade) with or without supplemented X-alpha-Gal and aureobasidin. The bait (MKKK18) did not autoactivate the reporter genes in yeast. **B.** Detection of ABI1/2 and MKKK18 expression in diploid yeast strains. Expression of BD- and AD-fusion proteins in yeast was determined by immunoblotting using specific anti-ABI1, anti-ABI2, and anti-MKKK18 antibodies. **C-D**. Pull-down assays to verify the interaction of ABI1/2 with MKKK18. Input lines represent 100% of the ABI1/2. Recombinant GST-MKKK18 or His-MKKK18 were pre-coupled to glutathione sepharose, and incubated with StrepTag-ABI1 or StrepTag-ABI2, respectively. Pulled-down StrepTagged ABI1 protein was detected (IB) with the epitope tag antibody. The presence of recombinant protein was confirmed using anti-MKKK18 antibody. **E-F.** ABI1-MKKK18 interaction occurs within the nucleus. BiFC analysis in Arabidopsis protoplasts expressing full-length ABI1/2 and MKKK18 fused to cECFP or nVenus, respectively. RFP

(E) was used as a transformation control. CFP-CBP20 (F) was used as a marker of nuclear localization.

Figure 7. ABI1 inhibits MKKK18 activity

A. Phosphatase activity of recombinant ABI1 and ABI2 proteins. The enzyme reactions were performed in 50 μl final volume containing 3–5 μg of GST-ABI1 or GST-ABI2. The results presented are the means from three independent biological replicates. **B.** ABI1 inactivates MKKK18. The MKKK18-GFP immunocomplex was incubated with 3 μg GST-ABI1 and GST-ABI2 (as a negative control), then the kinase activity was determined with MBP as a substrate. Equal loading was confirmed by CBB staining of MBP. The ^{32}P-labeled MBP bands were quantified and then normalized by the intensities of the corresponding control band using ImageJ software. Data are means ± SD of the relative band intensities from three independent experiments. An asterisk (*) indicates statistically significant changes determined using Student's *t*-test. **C–E**. Recombinant MKKK18 has no autophosphorylation activity *in vitro*. **C**. GST-MKKK18 was incubated with artificial (MBP) or/and *in vivo* substrate MKK3, without or in the presence of ^{32}P-ATP. Bands of GST-MKKK18, MKK3-GST and GST-SnRK2.6 are indicated by a close circle, a triangle, and an arrow, respectively. **D-E.** Effect of ABI1 on MKKK18 activity. Affinity-purified GST-MKKK18 was incubated with or without ABI1 (or ABI2). Kinase activity was monitored using *in vitro* (D) or with in-gel kinase activity assay, using MBP as substrate (E). Equal protein loading was confirmed by CBB staining. Immunoblotting confirmed the presence of GST fusion proteins. The blots shown are representative of three independent trials.

Figure 8. MKKK18 activity increases in the *abi1td* mutant in response to ABA treatment

A. Seedlings of WT Col-0, the *abi1td* and the *snrk2.6* mutants were treated with 100 μM ABA for the indicated times. A 600 μg aliquot of total protein was used for the immune complex MKKK18 activity assay using anti-MKKK18 antibody. CBB staining of MBP confirmed equal loading. Due to low abundance the endogenous MKKK18 protein was not detectable by immunoblot analysis. The results shown are representative of three independent experiments (n=9) with consistent results. **B.** ^{32}P-labeled MBP bands were quantified using ImageJ software and normalized by taking the radioactivity of the band in the absence of ABA as 1. Data are means ± SD of the relative band intensities from three independent experiments (n=9).

Figure 9. Proteasome-dependent degradation of MKKK18 is ABA-dependent and regulated by ABI1

A. qRT-PCR analysis of MKKK18 transcript accumulation in response to 50uM ABA for 90 min. in WT Col-0, *MKKK18oex*, *abi1td* and *abi1-2*. *MKKK18* expression levels were determined using three biological replicates and were normalized against 18S rDNA. The results are displayed as mean log2 fold change ± SE (n = 9) of three independent experiments with consistent results. **B.** MKKK18 stability in the cell-free degradation assay. GST-MKKK18 was incubated with 100 μg protein extract from either WT Col-0 or *abi1td* protoplasts incubated with or without 100 μM MG132 for 6 h in the dark. GST-MKKK18 protein levels at the indicated time points were determined by immunoblotting using GST antibodies. Ponceau S staining confirmed equal loading. **C-D.** Half-life plot for cell-free degradation of MKKK18 in WT Col-0 (B) and *abi1td* (C) extracts. Immunoblot images from each experiment were recorded simultaneously using a G:BOX Chemi XR5 fluorescence and chemiluminescence imaging system (Syngene) and the results were quantified using ImageJ

software. **E.** CHX treatment suppresses accumulation of MAPKKK18. Arabidopsis protoplasts expressing 35S:MAPKKK18-GFP were treated with mock, 3mM CHX, 3mM CHX and 100uM MG132. Blot is representative of four trials. MKKK18-GFP protein levels were determined by immunoblotting using anti-GFP antibodies. Ponceau S staining confirmed equal loading. MKKK18 protein bands were quantified using ImageJ software and normalized to the control (mock) band (set as 1). **F.** MKKK18 protein levels are affected by ABA. GST-MKKK18 was incubated with 100 μg total protein extract isolated from either WT Col-0 incubated with or without 50 μM ABA for 3 h in the dark. GST-MKKK18 protein levels at the indicated time points were determined by immunoblotting using GST antibodies. Ponceau S staining confirmed equal loading. MKKK18 protein bands were quantified using ImageJ software and normalized to the control band (set as 1).

Figure 10. Regulation of MKKK18 activity and stability by ABI1 PP2C

Under standard conditions, active ABI protein phosphatase inhibits MKKK18 kinase activity and protein stability. ABA receptors and dephosphorylated MKKK18 are directed for degradation via the proteasome pathway. In the presence of ABA, ABI1 PP2C activity is restrained by binding to the ABA-PYR complex (ABA signaling is turned on). Active MKKK18 activates the downstream cascade. ABA inhibits the degradation of ABA receptors by limiting their polyubiquitination.

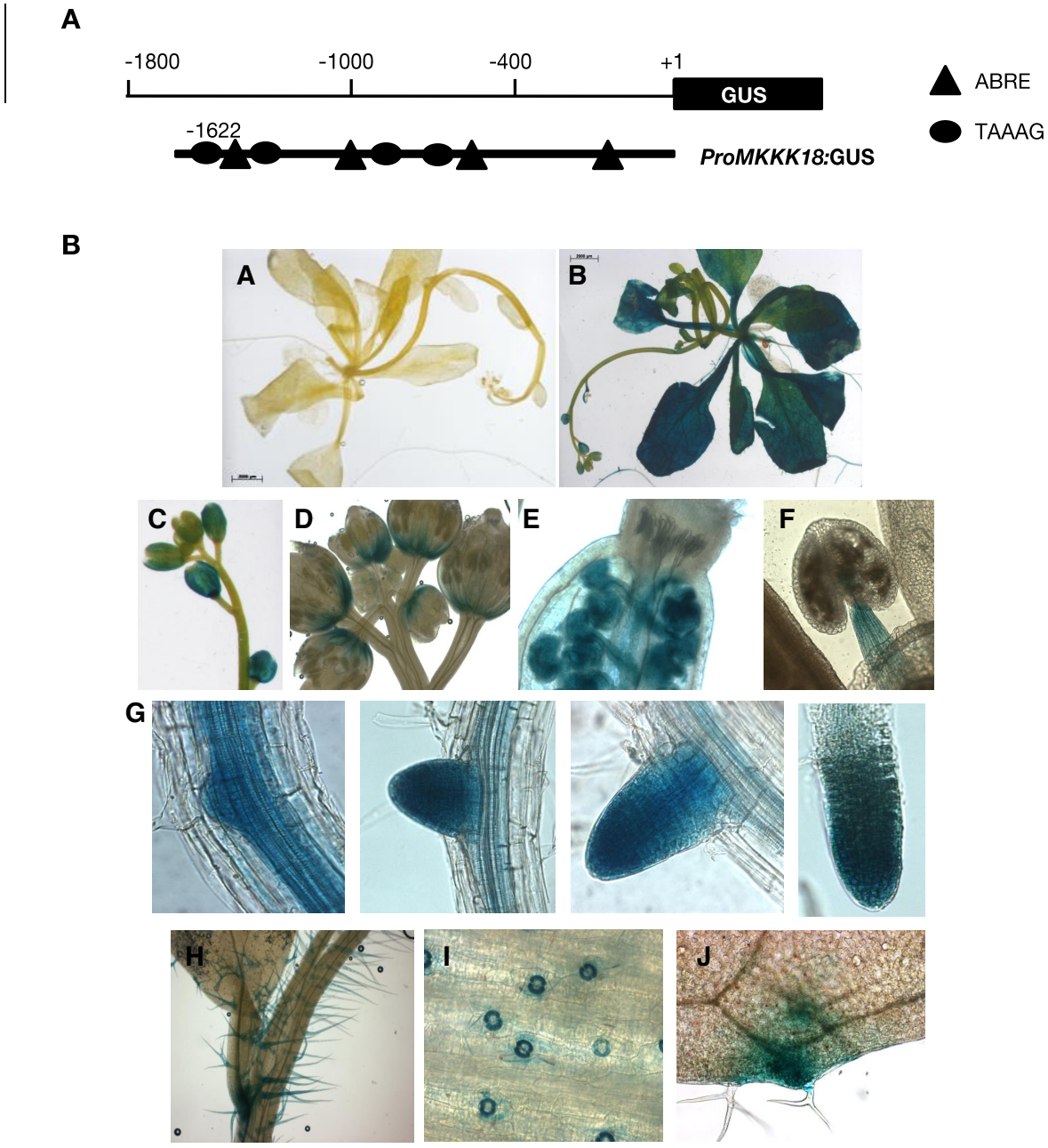
A
-1800
-1000
-400
+1
GUS
-1622
ProMKKK18:GUS
ABRE
TAAAG
B
A
B
C
D
E
F
G
H
I
J

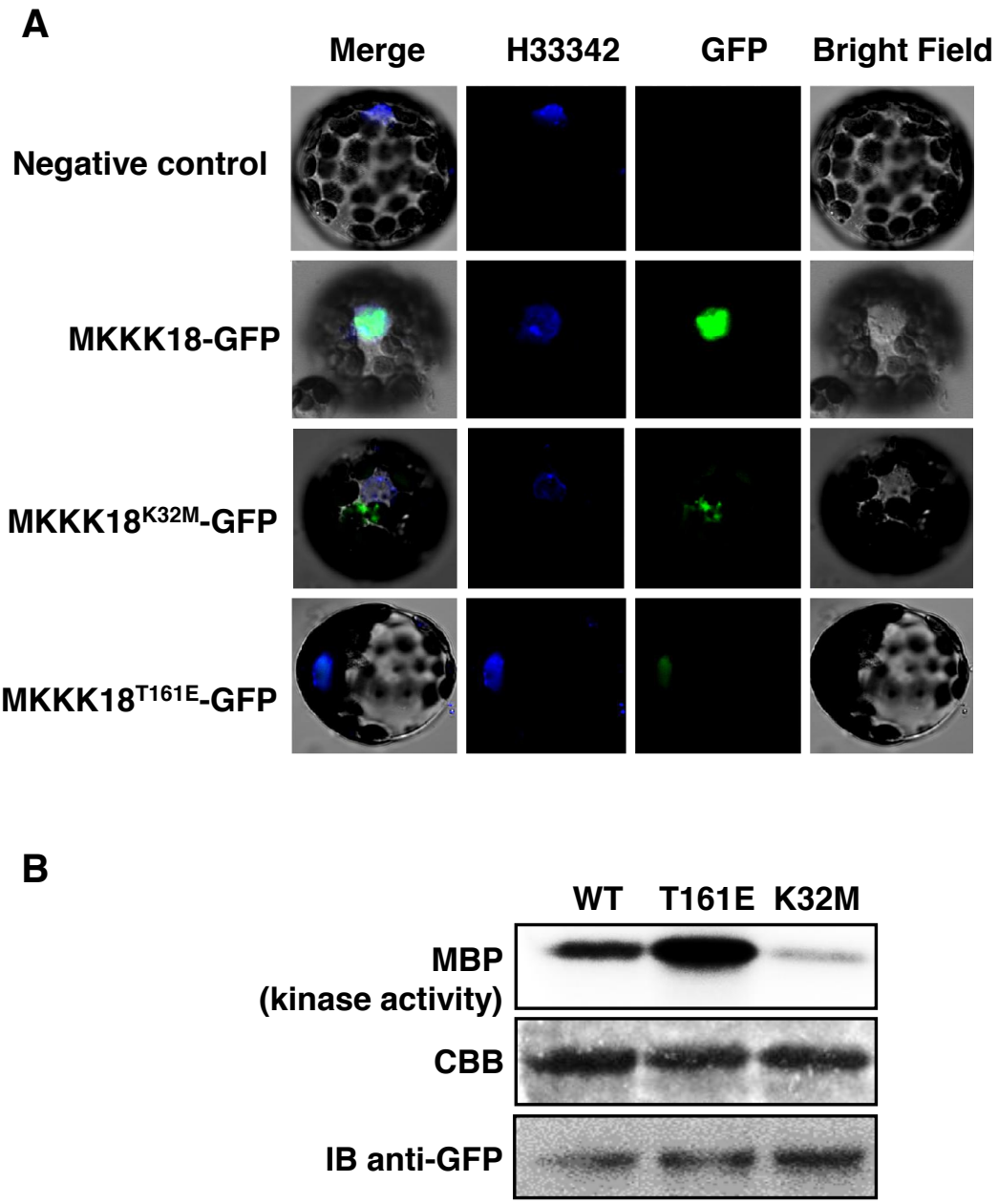
A
Merge
H33342
GFP
Bright Field
Negative control
MKKK18-GFP
MKKK18K32M-GFP
MKKK18T161E-GFP
B
WT
T161E
K32M
MBP
(kinase activity)
CBB
IB anti-GFP

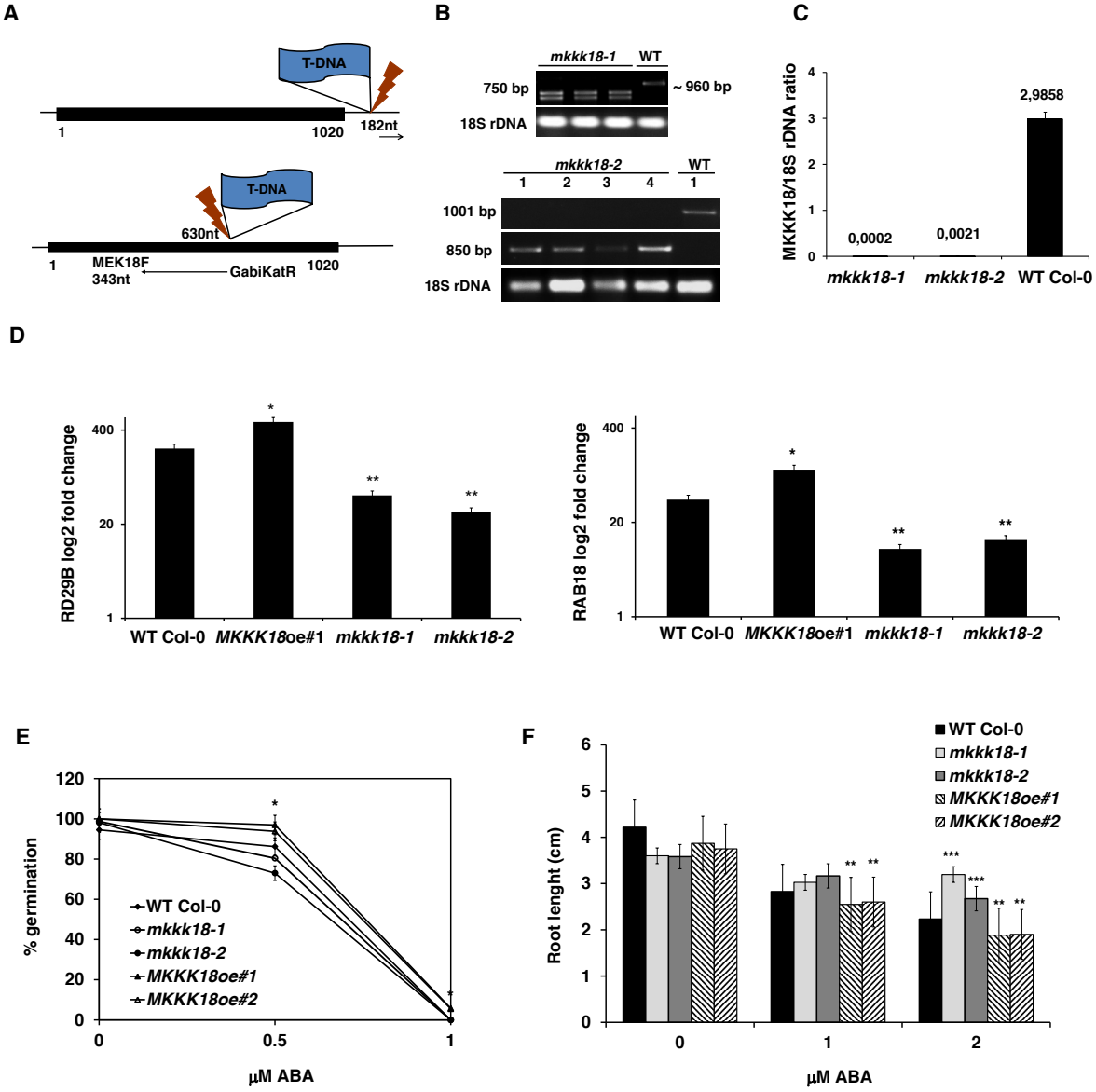
A
T-DNA
1
1020
182nt
T-DNA
630nt
1
MEK18F
343nt
GabiKatR
1020
B
mkkk18-1
WT
750 bp
~ 960 bp
18S rDNA
mkkk18-2
WT
1 2 3 4
1
1001 bp
850 bp
18S rDNA
C
MKKK18/18S rDNA ratio
0,0002
0,0021
2,9858
mkkk18-1
mkkk18-2
WT Col-0
D
RD29B log2 fold change
WT Col-0
MKKK18oe#1
mkkk18-1
mkkk18-2
RAB18 log2 fold change
WT Col-0
MKKK18oe#1
mkkk18-1
mkkk18-2
E
% germination
WT Col-0
mkkk18-1
mkkk18-2
MKKK18oe#1
MKKK18oe#2
µM ABA
F
Root lenght (cm)
WT Col-0
mkkk18-1
mkkk18-2
MKKK18oe#1
MKKK18oe#2
µM ABA

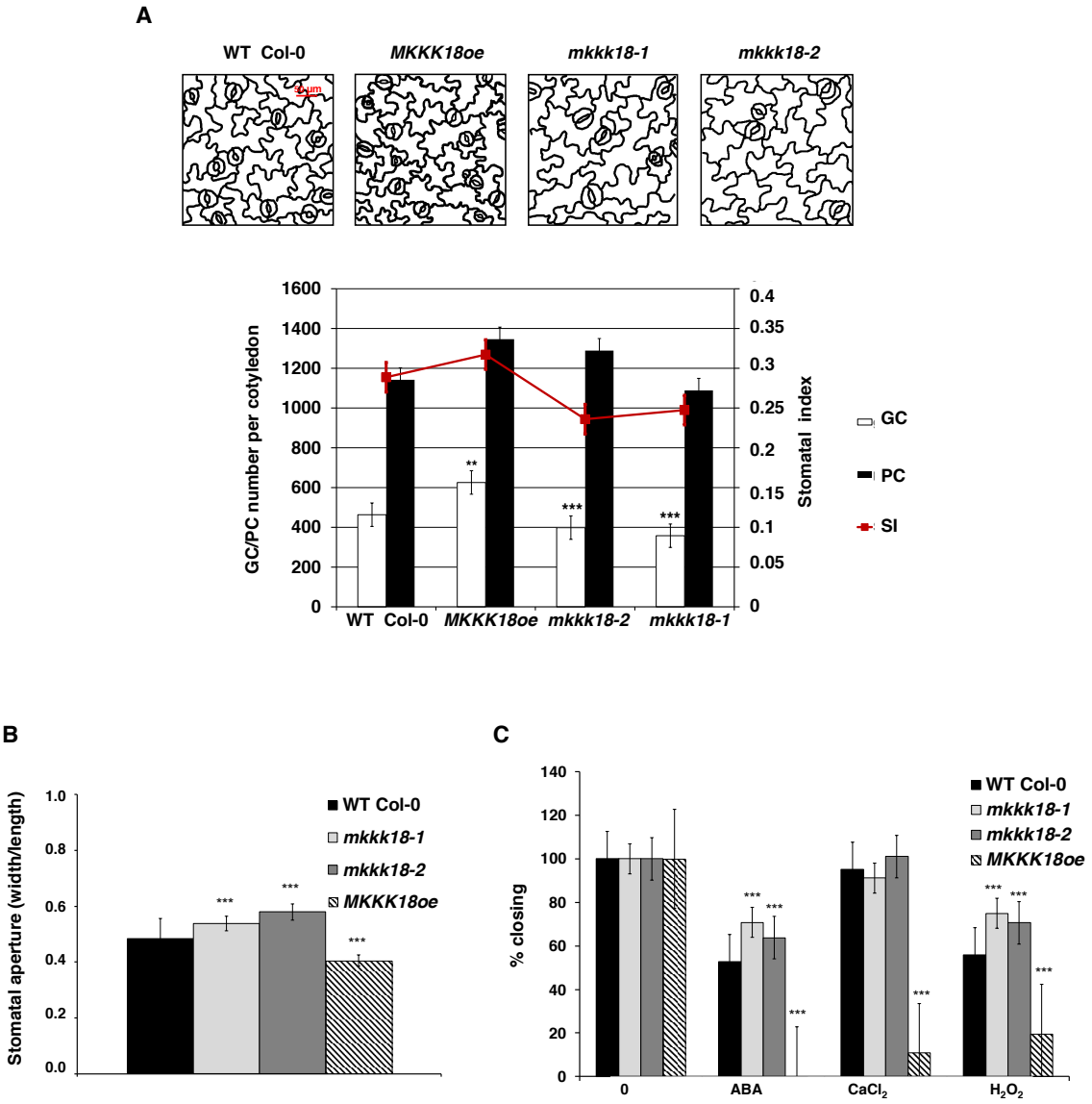
A
WT Col-0
MKKK18oe
mkkk18-1
mkkk18-2
5μm
GC/PC number per cotyledon
Stomatal index
GC
PC
SI
WT Col-0
MKKK18oe
mkkk18-2
mkkk18-1
B
Stomatal aperture (width/length)
WT Col-0
mkkk18-1
mkkk18-2
MKKK18oe
C
% closing
0
ABA
CaCl2
H2O2

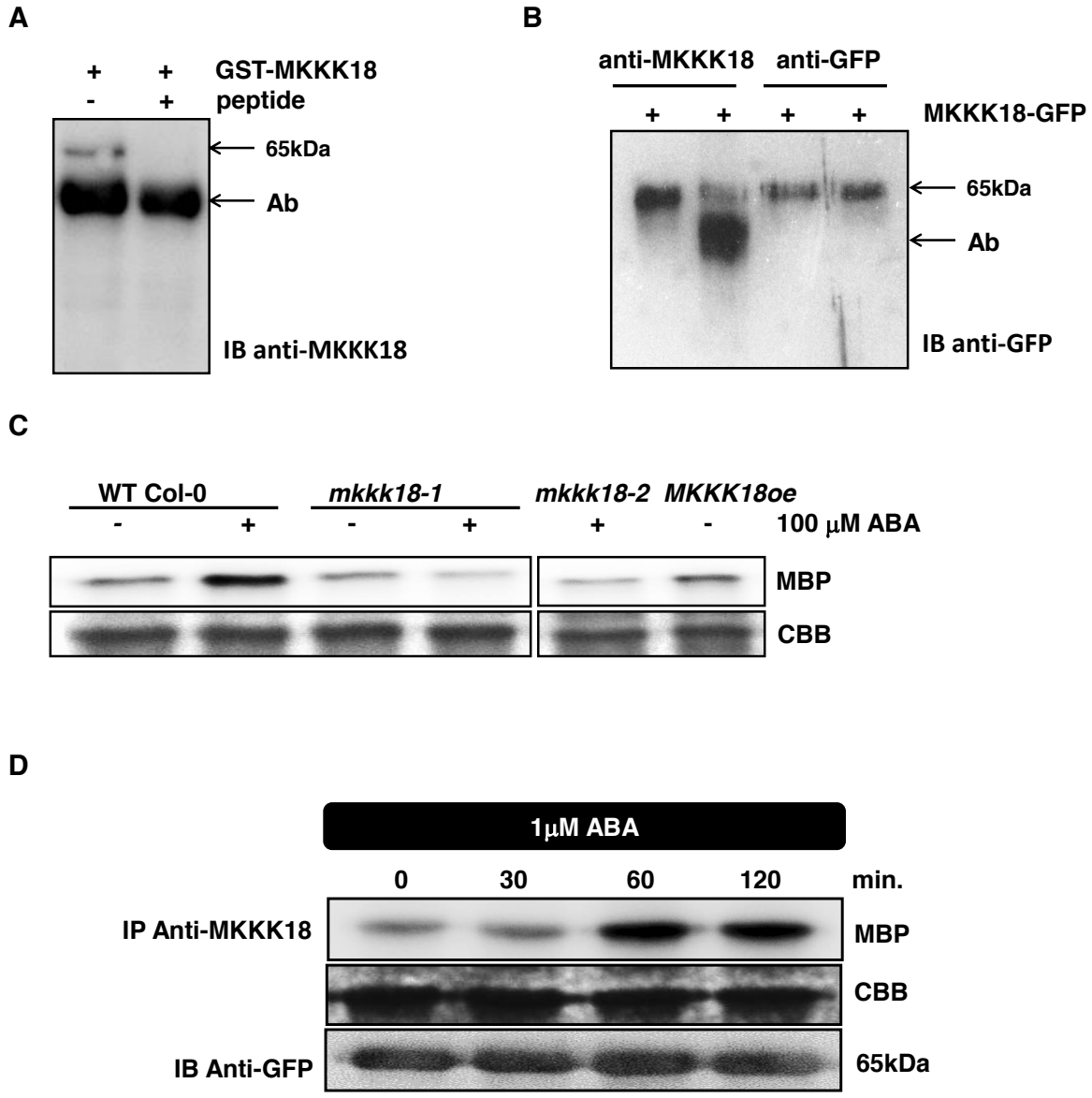
A
+ + GST-MKKK18
- + peptide
65kDa
Ab
IB anti-MKKK18
B
anti-MKKK18 anti-GFP
+ + + + MKKK18-GFP
65kDa
Ab
IB anti-GFP
C
WT Col-0 mkkk18-1 mkkk18-2 MKKK18oe
- + - + + - 100 μM ABA
MBP
CBB
D
1μM ABA
0 30 60 120 min.
IP Anti-MKKK18
MBP
CBB
IB Anti-GFP
65kDa

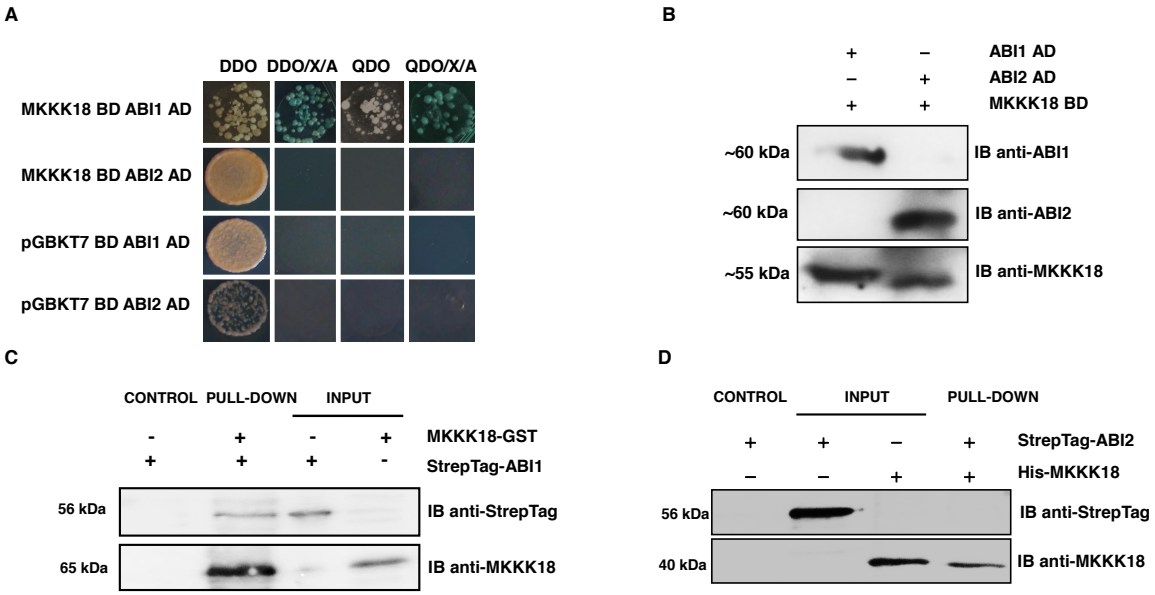
A
DDO
DDO/X/A
QDO
QDO/X/A
MKKK18 BD ABI1 AD
MKKK18 BD ABI2 AD
pGBKT7 BD ABI1 AD
pGBKT7 BD ABI2 AD
B
ABI1 AD
ABI2 AD
MKKK18 BD
~60 kDa
IB anti-ABI1
~60 kDa
IB anti-ABI2
~55 kDa
IB anti-MKKK18
C
CONTROL
PULL-DOWN
INPUT
MKKK18-GST
StrepTag-ABI1
56 kDa
IB anti-StrepTag
65 kDa
IB anti-MKKK18
D
CONTROL
INPUT
PULL-DOWN
StrepTag-ABI2
His-MKKK18
56 kDa
IB anti-StrepTag
40 kDa
IB anti-MKKK18

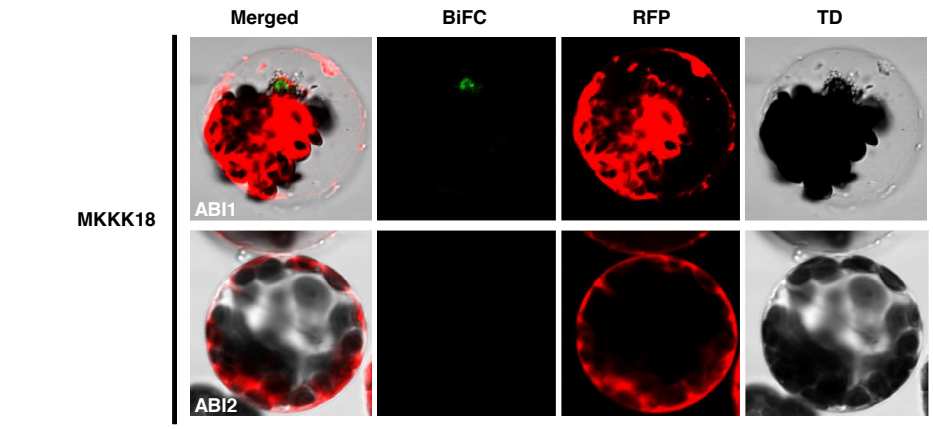
E
Merged
BiFC
RFP
TD
MKKK18
ABI1
ABI2

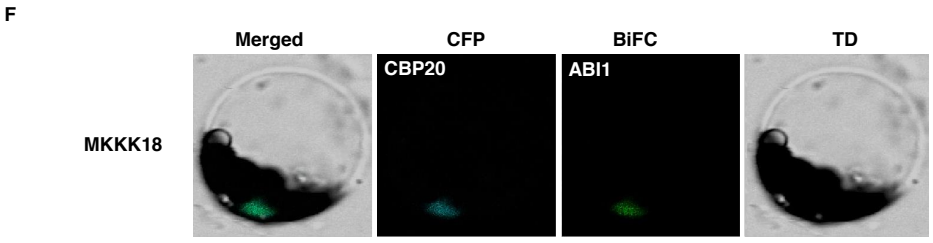
F
Merged
CFP
BiFC
TD
MKKK18
CBP20
ABI1

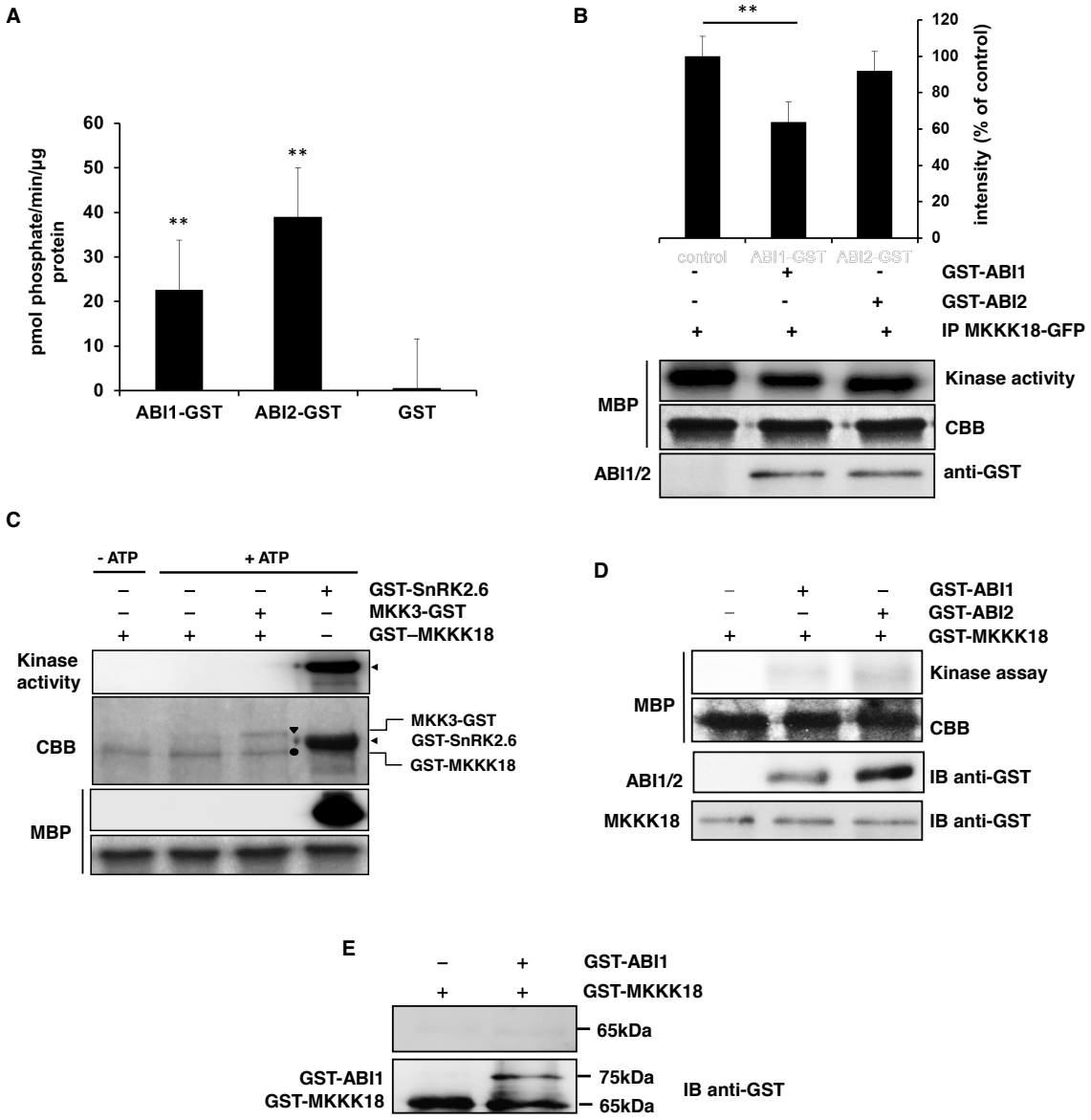
A
pmol phosphate/min/µg protein
60
50
40
30
20
10
0
**
**
ABI1-GST
ABI2-GST
GST
B
**
120
100
80
60
40
20
0
intensity (% of control)
control
ABI1-GST
ABI2-GST
GST-ABI1
GST-ABI2
IP MKKK18-GFP
MBP
Kinase activity
CBB
ABI1/2
anti-GST
C
- ATP
+ ATP
GST-SnRK2.6
MKK3-GST
GST–MKKK18
Kinase activity
CBB
MBP
MKK3-GST
GST-SnRK2.6
GST-MKKK18
D
GST-ABI1
GST-ABI2
GST-MKKK18
MBP
Kinase assay
CBB
ABI1/2
IB anti-GST
MKKK18
IB anti-GST
E
GST-ABI1
GST-MKKK18
65kDa
GST-ABI1
GST-MKKK18
75kDa
65kDa
IB anti-GST

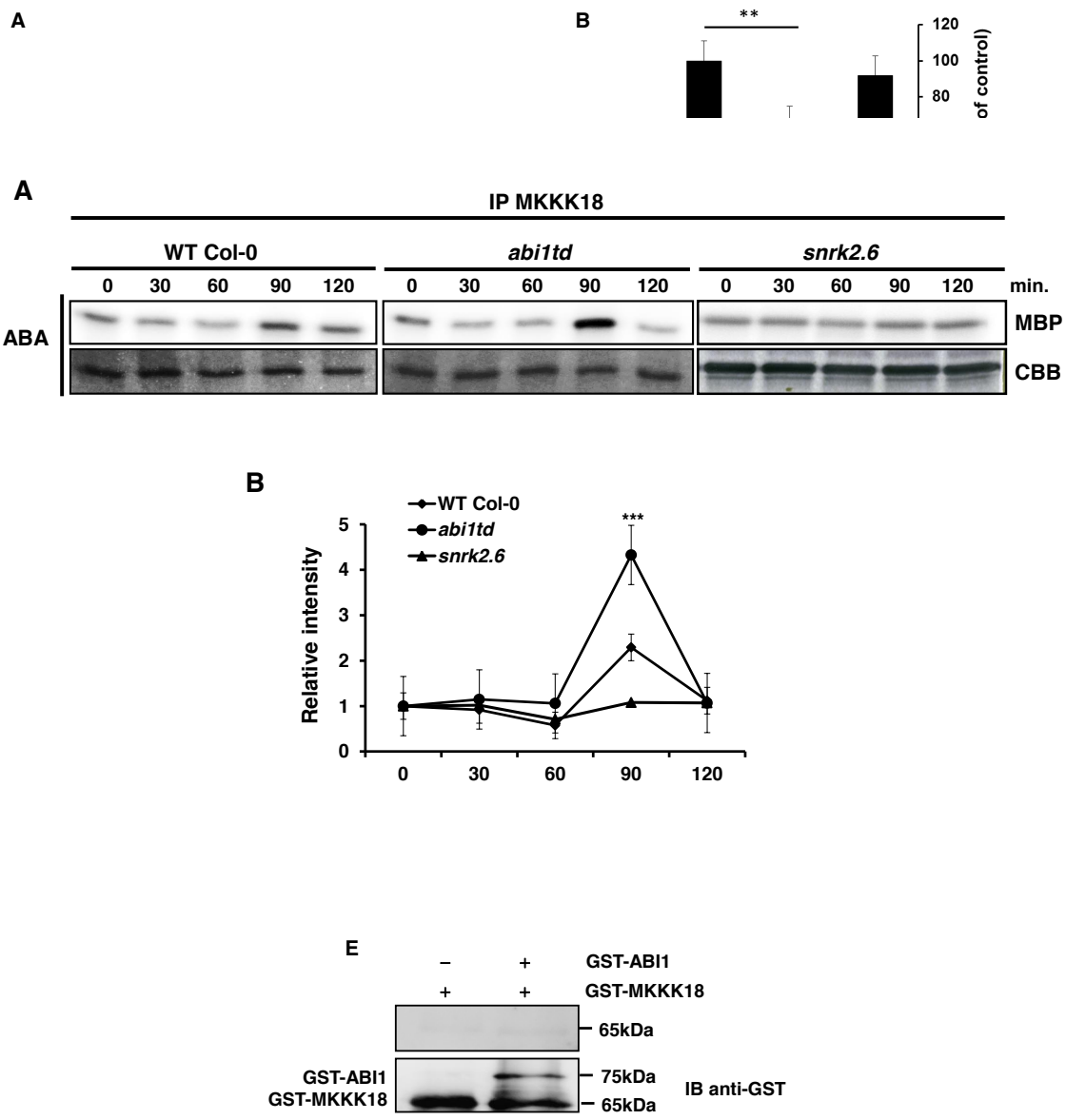
A
B
**
120
100
80
of control)
A
IP MKKK18
WT Col-0
abi1td
snrk2.6
0 30 60 90 120 0 30 60 90 120 0 30 60 90 120 min.
ABA
MBP
CBB
B
WT Col-0
abi1td
snrk2.6
***
Relative intensity
5
4
3
2
1
0
0 30 60 90 120
E
– + GST-ABI1
+ + GST-MKKK18
65kDa
GST-ABI1
GST-MKKK18
75kDa
65kDa
IB anti-GST

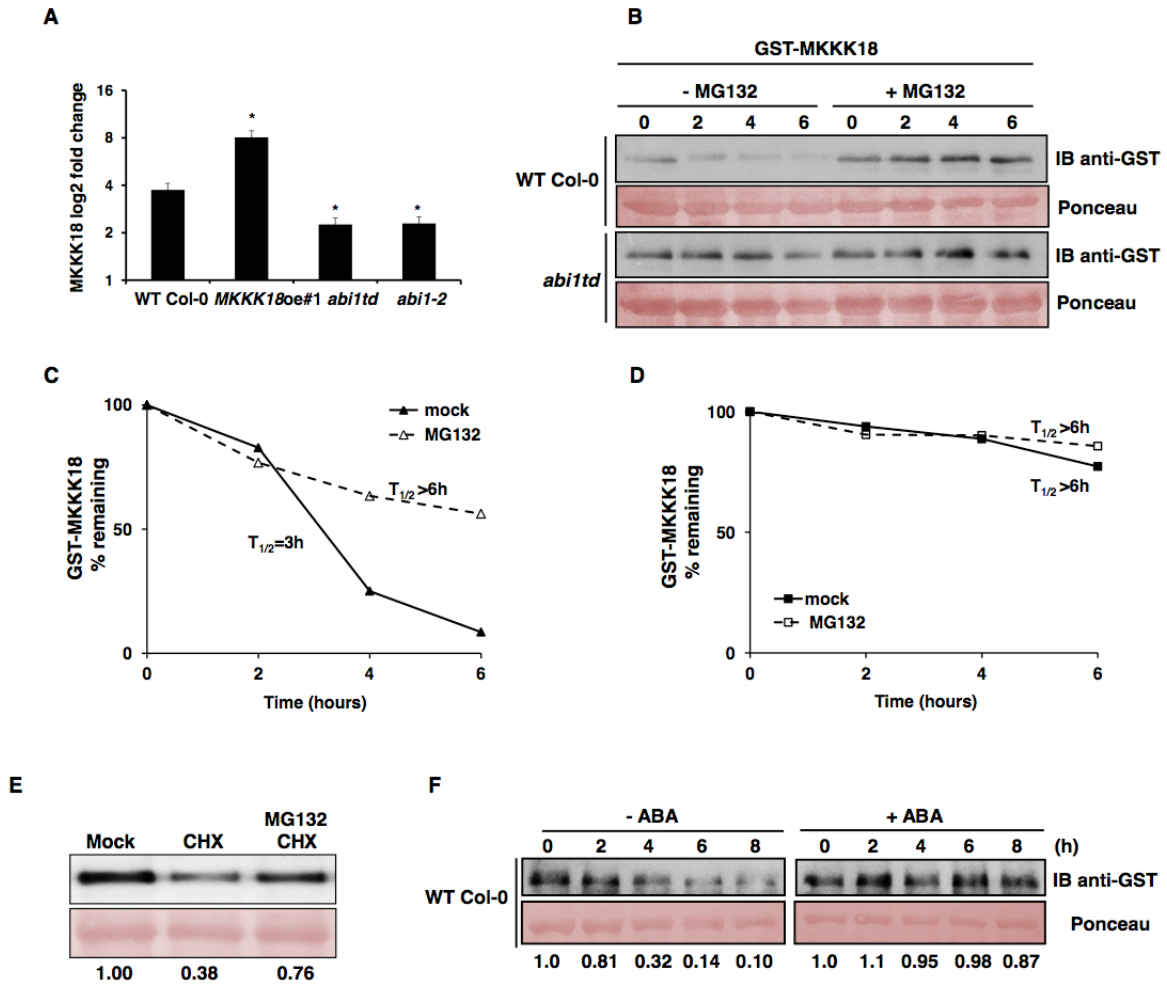
A
MKKK18 log2 fold change
16
8
4
2
1
WT Col-0
MKKK18oe#1
abi1td
abi1-2
B
GST-MKKK18
- MG132
+ MG132
0 2 4 6 0 2 4 6
WT Col-0
IB anti-GST
Ponceau
abi1td
IB anti-GST
Ponceau
C
GST-MKKK18 % remaining
100
50
0
mock
MG132
T1/2>6h
T1/2=3h
0 2 4 6
Time (hours)
D
GST-MKKK18 % remaining
100
50
0
T1/2>6h
T1/2>6h
mock
MG132
0 2 4 6
Time (hours)
E
Mock
CHX
MG132 CHX
1.00 0.38 0.76
F
- ABA
+ ABA
0 2 4 6 8 0 2 4 6 8 (h)
WT Col-0
IB anti-GST
Ponceau
1.0 0.81 0.32 0.14 0.10 1.0 1.1 0.95 0.98 0.87

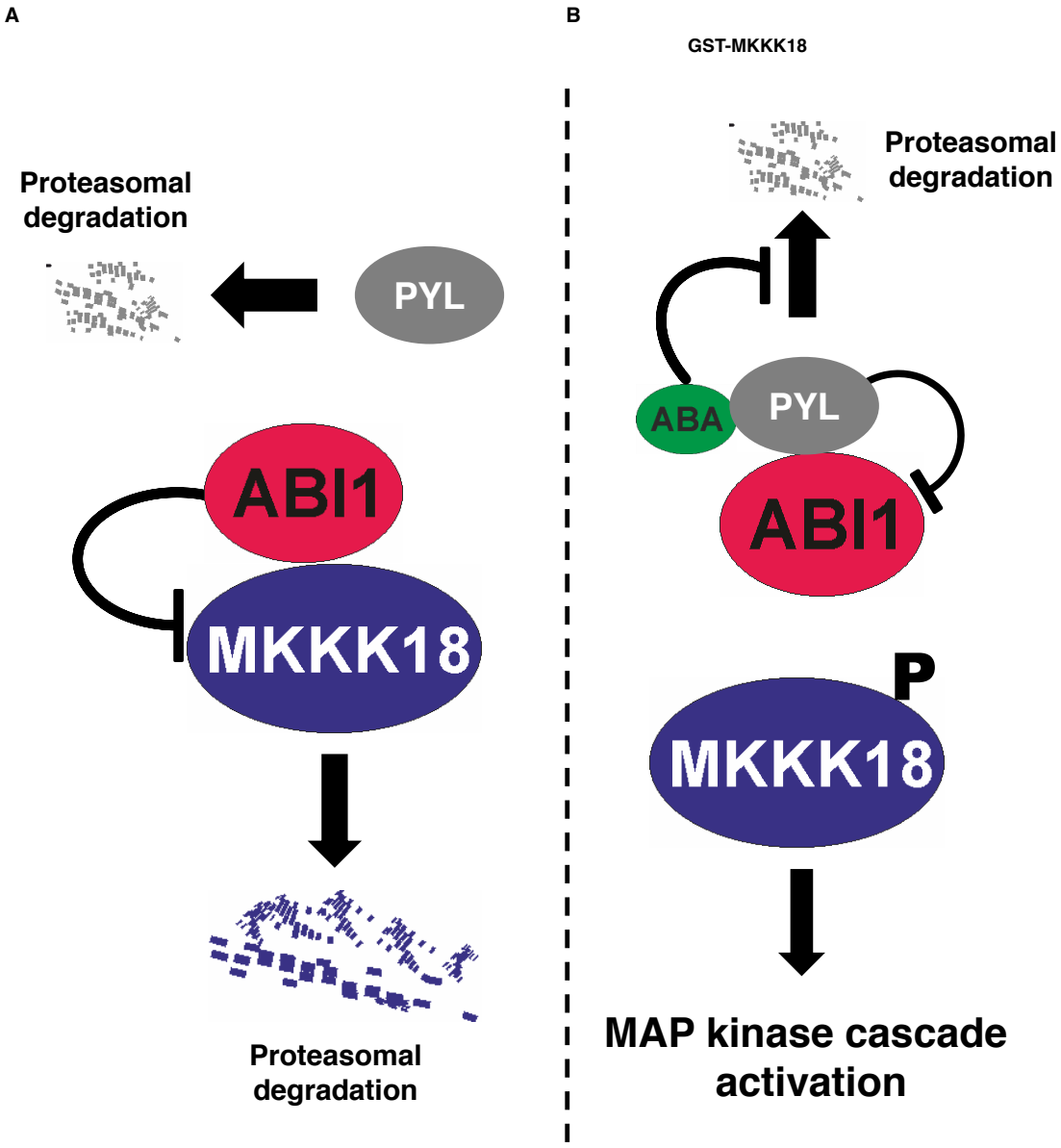
A
Proteasomal degradation
PYL
ABI1
MKKK18
Proteasomal degradation
B
GST-MKKK18
Proteasomal degradation
ABA
PYL
ABI1
P
MKKK18
MAP kinase cascade activation